DOI: 10.1534/genetics.106.067116

The Plexin PLX-2 and the Ephrin EFN-4 Have Distinct Roles in MAB-20/Semaphorin 2A Signaling in *Caenorhabditis elegans* Morphogenesis

Fumi Nakao,*[,1] Martin L. Hudson,[†,1] Motoshi Suzuki,* Zachary Peckler,[†] Rie Kurokawa,* Zhicen Liu,* Keiko Gengyo-Ando,[‡] Akira Nukazuka,* Takashi Fujii,* Fumikazu Suto,* Yukimasa Shibata,* Go Shioi,* Hajime Fujisawa,* Shohei Mitani,[‡] Andrew D. Chisholm[†] and Shin Takagi*[,2]

*Division of Biological Science, Nagoya University Graduate School of Science, Chikusa-ku, Nagoya 464-8602, Japan, [†]Department of Molecular, Cell and Developmental Biology, Sinsheimer Laboratories, University of California, Santa Cruz, California 95064 and [‡]Department of Physiology, Tokyo Women's Medical University School of Medicine, Tokyo 162-8666, Japan

Manuscript received October 21, 2006
Accepted for publication April 24, 2007

ABSTRACT

Semaphorins are extracellular proteins that regulate axon guidance and morphogenesis by interacting with a variety of cell surface receptors. Most semaphorins interact with plexin-containing receptor complexes, although some interact with non-plexin receptors. Class 2 semaphorins are secreted molecules that control axon guidance and epidermal morphogenesis in Drosophila and *Caenorhabditis elegans*. We show that the *C. elegans* class 2 semaphorin MAB-20 binds the plexin PLX-2. *plx-2* mutations enhance the phenotypes of hypomorphic *mab-20* alleles but not those of *mab-20* null alleles, indicating that *plx-2* and *mab-20* act in a common pathway. Both *mab-20* and *plx-2* mutations affect epidermal morphogenesis during embryonic and in postembryonic development. In both contexts, *plx-2* null mutant phenotypes are much less severe than *mab-20* null phenotypes, indicating that PLX-2 is not essential for MAB-20 signaling. Mutations in the ephrin *efn-4* do not synergize with *mab-20*, indicating that EFN-4 may act in MAB-20 signaling. EFN-4 and PLX-2 are coexpressed in the late embryonic epidermis where they play redundant roles in MAB-20-dependent cell sorting.

SEMAPHORINS are secreted molecules first identified as axon guidance cues causing growth cone collapse (Fan *et al.* 1993; Kolodkin *et al.* 1993). Semaphorins have subsequently been shown to play myriads of roles in neural and non-neural development, including cell migration (Kruger *et al.* 2005), tissue morphogenesis (Hinck 2004), formation of the vascular system (Suchting *et al.* 2006), and regulation of the immune system (Takegahara *et al.* 2005). The semaphorin family comprises a large number of secreted and transmembrane proteins sharing the signature sema domain of 500 amino acid residues (Semaphorin Nomenclature Committee 1999). Semaphorins have been classified by domain architecture and by sequences of their sema domains (Kolodkin *et al.* 1993). Classes 1 and 2 are invertebrate specific, whereas classes 3, 4, and 7 are found only in vertebrates; class 5 is found in both vertebrates and invertebrates. Class 2 semaphorins are composed of an N-terminal sema domain, a cysteine-rich domain, and a C-terminal immunoglobulin domain; interestingly, class 2 semaphorins do not contain motifs mediating membrane attachment, yet appear to function as short-range signals. Expression of Drosophila Sema II/Sema-2a on specific muscles causes them to repel axonal growth cones (Matthes *et al.* 1995; Winberg *et al.* 1998). Sema-2a also acts at short range to repel larval sensory neurons (Bates and Whitington 2007). In contrast, Sema-2a is a long-range chemorepulsive guidance cue in grasshoppers (Isbister *et al.* 1999, 2003). In *Caenorhabditis elegans*, the class 2 semaphorin MAB-20 promotes separation between epidermal cells (Roy *et al.* 2000); it is not known whether this reflects a long- or short-range role for MAB-20, which is widely expressed.

Semaphorins interact with a remarkably diverse set of cell surface receptors. One major class of cell surface receptors are the plexins, transmembrane proteins first identified as antigens expressed in restricted regions in the nervous system (Ohta *et al.* 1992, 1995; Kameyama *et al.* 1996a,b; Fujisawa *et al.* 1997) and as molecules with a Met-related motif (Maestrini *et al.* 1996). Some transmembrane semaphorins, such as the invertebrate class 1 semaphorins, directly bind plexins (Winberg *et al.* 1998). Plexins themselves contain an N-terminal sema domain that binds the sema domain of the semaphorin. Plexins also contain cysteine-rich repeats known

[1]These authors contributed equally to this work.

[2]*Corresponding author:* Division of Biological Science, Nagoya University Graduate School of Science, Furo-cho, Chikusa-ku, Nagoya 464-8602, Japan. E-mail: i45116a@nucc.cc.nagoya-u.ac.jp

as Met-related sequences (MRS) or plexin/semaphorin/integrin domains and three glycine–proline-rich (GP) repeats; the roles of these domains are not well understood. Class 3 semaphorins interact with receptor complexes composed of plexins and neuropilins (Tamagnone *et al.* 1999). In such receptor complexes, semaphorins bind the neuropilin subunit whereas the plexin is essential for signal transduction into the cell via its cytoplasmic domain. In addition to neuropilins, plexins can act in receptor complexes with a variety of membrane proteins (Pasterkamp and Kolodkin 2003). Finally, some semaphorins can signal independently of plexins (Pasterkamp *et al.* 2003). The signaling pathways and receptors for several semaphorin classes remain to be fully elucidated. Here we report a genetic analysis of factors acting in the *C. elegans* class 2 semaphorin MAB-20 pathway.

C. elegans encodes two class 1 transmembrane semaphorins (SMP-1/Ce-sema-1a and SMP-2/Ce-sema-1b), and one class 2 semaphorin (MAB-20/Ce-sema-2a) (Roy *et al.* 2000). *C. elegans* also encodes two plexins, the plexin A family member PLX-1 and PLX-2 described here. Compared with vertebrates, in which >20 semaphorins and at least nine plexins are present, the relative simplicity of the *C. elegans* semaphorin/plexin signaling system allows systematic tests of their ligand-receptor relationships *in vivo*. We previously showed that PLX-1 binds to SMP-1, but not to MAB-20 (Fujii *et al.* 2002). Genetic analysis indicates that SMP-1 and SMP-2 play redundant roles in a pathway that involves PLX-1 (Ginzburg *et al.* 2002) and that PLX-1 signaling may be attractive or repulsive, depending on context (Dalpe *et al.* 2004, 2005).

Mutations in *mab-20* cause abnormal embryonic epidermal morphogenesis and defects in embryonic migrations of ventral neuroblasts that may contribute to epidermal defects (Roy *et al.* 2000; Chin-Sang *et al.* 2002). *mab-20* mutants also display aberrant morphogenesis of sensilla (rays) in the adult male tail (Baird *et al.* 1991). The neurons and structural cells of each ray form a three-cell group derived from precursors known as Rn.a cells. In *mab-20* males, adjacent rays display fusion, in which cells of one ray associate with those of a neighboring ray to form a single large ray (Baird *et al.* 1991). The ray fusion phenotypes of *mab-20* mutants have been interpreted as resulting from inappropriate adhesion between ray cells of adjacent groups (Roy *et al.* 2000). It is not yet understood at the cellular level how MAB-20 regulates the cell rearrangements that result in distinct ray groups. As MAB-20 is broadly expressed, it may act as a permissive signal that prevents inappropriate cell contacts and thus allows sorting of cell groups. To address these questions, it is critical to define the receptors that mediate MAB-20 functions.

MAB-20 does not bind PLX-1, so an obvious candidate for the MAB-20 receptor is the other *C. elegans* plexin, PLX-2. Indeed, mutations in *plx-2* enhance ray fusion defects of weak *mab-20* alleles (Ikegami *et al.* 2004). However, physical interactions between MAB-20 and PLX-2 have not been tested, and their interactions in embryogenesis have not been described. Here we show that PLX-2 binds MAB-20, consistent with a receptor–ligand relationship. Different parts of the PLX-1 and PLX-2 extracellular domains are involved in binding semaphorins, suggesting that the signaling mechanisms of class 1 and class 2 semaphorins may differ. Surprisingly, *plx-2* deletion mutations isolated by reverse genetics display very weak morphogenetic phenotypes compared to *mab-20* mutants, suggesting that MAB-20 interacts with additional receptors. One candidate for an additional component of the MAB-20 pathway is the ephrin EFN-4, which functions in morphogenesis independently of the Eph receptor VAB-1 (Chin-Sang *et al.* 2002). *efn-4* mutants resemble *mab-20* mutants in many phenotypes, and *efn-4* mutations do not enhance some *mab-20* mutant phenotypes (Chin-Sang *et al.* 2002; Ikegami *et al.* 2004). It is unclear how an ephrin might contribute to semaphorin signaling, and further analysis of this unusual interaction has awaited the identification of the MAB-20 receptor. Our genetic analysis indicates that PLX-2 and EFN-4 have partly redundant roles in a subset of MAB-20 functions.

MATERIALS AND METHODS

Genetics: *C. elegans* culture and genetic manipulations used standard procedures (Brenner 1974). *C. elegans* strains N2, DR466 *him-5(e1490) LGV*, EM67 *mab-20(bx24) LGI; him-5(e1490)*, EM253 *mab-20(bx61); him-5(e1490)*, EM305 *efn-4 (bx80) LGIV; him-5(e1490)*, and NL2099 *rrf-3(pk1426)LGII* were obtained from the Caenorhabditis Genetics Center, care of T. Stiernagle (University of Minnesota). Time-lapse analysis of embryogenesis was performed on the following strains: CZ977 *efn-4(bx80)*, CZ1724 *mab-20(ev574)*, CZ4859 *plx-2(tm729) LGII*, ST71 *tm729; bx80*, ST72 *ev574; tm729*, ST73 *ev574; bx80*, ST74 *ev574; tm729; bx80*, and CZ5784 *plx-2(nc7). ncIs13* is an integrant of AJM-1::GFP (Liu *et al.* 2005). Genotypes of all double mutants except those containing *bx61* were confirmed by PCR; primer sequences and the conditions for PCR are available on request.

To determine the penetrance of embryonic lethality, eggs that failed to hatch within 2 days after being laid were scored as embryonic arrest. All estimates of penetrance were obtained from between 5 and 17 complete broods. One-way ANOVA was used to compare differences in penetrance.

Molecular biology of *plx-2*: The cDNA clone yk21h1 encoding the C-terminal 1103 residues of PLX-2 was isolated by Y. Kohara's group. We constructed a full-length *plx-2* cDNA by combining yk21h1 and a 5′ RACE product amplified with a gene-specific primer and a primer corresponding to the trans-spliced leader SL1. DNA sequences were determined for both strands. Our composite *plx-2* cDNA sequence agrees with the Gene Summary for *plx-2* in the current version of Wormbase (WS157) and does not contain the "exon 1" reported by Ikegami *et al.* (2004).

To examine the expression of the *plx-2* gene, we made transcriptional and translational GFP reporter genes. The P*plx-2*-GFP transcriptional reporter SBB67 contains 10.9-kb genomic DNA 5′ to the *plx-2* ATG (nt 20,517–9566 of cosmid K04B12) cloned into pPD95.75 (provided by A. Fire) in two steps. A 10-kb *Bam*HI fragment of K04B12 (20,517–10,500) was cloned into

the *Bam*HI site of pPD95.75; the remaining 5′ region (10,500–9566) was amplified by PCR and inserted into pPD95.75. We made P*plx-2*-GFP arrays with the *rol-6(dm)* pRF4 coinjection marker; one array underwent spontaneous chromosomal integration during strain propagation, yielding *ncIs21* described here.

We made two translational fusion constructs. A full-length PLX-2::GFP translational fusion construct (KKB75) was made by subcloning genomic fragments of K04B12 into pPD95.75, except for the 3′ terminal fragment (3320–2675), which was amplified and cloned into the *Kpn*I site of pPD95.75. We coinjected KKB75 (0.2 μg/μl) with pRF4 to generate extrachromosomal arrays that were integrated by gamma-ray mutagenesis to create *ncIs30*. For the partial translational fusion construct, a PCR fragment corresponding to the *plx-2* genomic DNA, 20,517–6426 nt of K04B12, was cloned into *Bam*HI–*Sal*I-digested pFXneEGFP (S. Mitani, unpublished results), resulting in the translational fusion of the N-terminal half of PLX-2 (residues 1–888) with enhanced GFP (EGFP) (Living Colors Fluorescent Proteins, CLONTECH). All PCR-amplified fragments in the reporter constructs, except for that in the partial translational fusion construct, were sequenced. To examine GFP fluorescence, worms were mounted on 4% agarose containing 1 mm levamisole and were examined with a Zeiss Axioplan microscope using Zeiss filter set no. 10. Images were recorded with a camera (Coolpix 990, Nikon). We used anti-GFP immunostaining to analyze GFP reporter expression in embryos. Embryos were fixed and stained essentially as previously described (Hudson *et al.* 2006) and images were collected on a Zeiss Pascal confocal microscope. The full-length PLX-2::GFP translational fusion did not fluoresce at detectable levels; low levels of expression were detectable by anti-GFP immunostaining (not shown).

Isolation of *plx-2* deletion alleles: *nc7* was isolated by Tc1-transposon-mediated deletion mutagenesis using the mutator strain MT3126 according to a protocol described previously (Shibata *et al.* 2000). First, we isolated the mutation *nc8::Tc1* in which the Tc1 transposon is inserted at the position corresponding to nt 6617/6618 of cosmid K04B12 in intron 9 of *plx-2*. Then, a deletion allele, *nc7*, which deleted the fragment corresponding to 5596–7488 nt of cosmid K04B12, with the breakpoints of cccgagcacaccaat [*nc7*] ccatcgacaattgga, was isolated. The deletion *nc7* was confirmed by Southern blot analysis (data not shown). The deletion *tm729* was generated by chemical mutagenesis and isolated as described (Gengyo-Ando and Mitani 2000). *tm729* deletes nucleotides 7632–9291 of cosmid K04B12, with the breakpoints of cagagtgggtctaca [*tm729*] gagactaagcattct. Both mutations were outcrossed 10 times to N2 before analysis.

Time-lapse analysis of embryonic morphogenesis: Four-dimensional (4D) time-lapse microscopy of embryonic development was performed as described (George *et al.* 1998; Chin-Sang *et al.* 1999). We timed the following morphogenetic movements: (1) gastrulation, defined as the time from ingression of the E daughter cells to ingression of the germline and D lineage; (2) closure of the ventral cleft by lateral migrations of ventral neuroblasts (Hudson *et al.* 2006); (3) epidermal enclosure; (4) epidermal elongation to comma stage. At least 12 embryos were analyzed for each genotype in Figure 4, although not all time points were scorable in each embryo.

Analysis of male tail-ray morphology: We classified the arrangement of Rn.p epidermal cells in larval male tails into five classes for quantification. In class I, all Rn.ps adopted apparently wild-type morphology. In class II, R4.p adopted a triangular shape rather than a wild-type rectangular shape. In class III, R1/2.ps were larger or irregular in shape compared with the wild type. In class IV, animals exhibited both class II and class III defects simultaneously. In class V, morphology of all Rn.ps was abnormal.

RNA interference: A *plx-2* cDNA fragment (1–789 nt), a *plx-1* cDNA fragment (1–693 nt), a *smp-1* cDNA fragment (1–566 nt), a *smp-2* cDNA fragment (1289–1951 nt), and a *mab-20* cDNA fragment (1749–2240 nt) subcloned into pBluescript SK (Stratagene, La Jolla, CA) were amplified by PCR. The PCR products were used as templates for RNA synthesis with T7 RNA polymerase (Boehringer Mannheim, Indianapolis), and double-stranded RNAs were purified with an RNeasy kit (QIAGEN, Valencia, CA). RNA interference (RNAi) by soaking (Maeda *et al.* 2001) was performed in the genetic background of *rrf-3(pk1426)*, which causes hypersensitivity to RNAi (Simmer *et al.* 2002).

Binding analysis: cDNAs encoding mutant plexins were generated by PCR. PLX-2ΔMRS-GP deletes D(493)-Q(1067). PLX-1ΔMRS-GP deletes L(568)-P(1108). PLX-1Δsema deletes the N terminus up to R(496). PLX-1Δect deletes the N terminus up to P(1108). The wild-type and mutant plexin cDNA were inserted into pCAGGS (Niwa *et al.* 1991) and tagged with the c-*myc* epitope (GEQKLISEEDL) at the N terminus (Evan *et al.* 1985). In all the expression constructs used in the binding assay, a native signal sequence and sequences immediately upstream of the translation initiation codon for *C. elegans* proteins were replaced with that of a mouse Sema3A (1–25 aa) (Puschel *et al.* 1995) and a vertebrate Kozak consensus sequence (CCACC), respectively (Kozak 1992). The construction of Ce-Sema-1a-ΔC-Fc-AP and Ce-Sema-2a-Fc, containing the ecto-domain of SMP-1 and MAB-20, respectively, was described previously (Fujii *et al.* 2002).

To express EFN-4, we amplified cDNA corresponding to the entire coding region of *efn-4* using the cDNA clone yk449e2 as template and primers to introduce the first four residues of the signal sequence and appropriate restriction sites and cloned the resulting PCR product into the *Hin*dIII–*Bam*HI sites of pcDNA3 (Invitrogen, San Diego), creating plasmid pCZ152.

HEK293T cells were transfected with the expression constructs using Effectene transfection reagent (QIAGEN). Two days after transfection, culture medium containing Ce-Sema-1a-ΔC-Fc-AP or Ce-Sema-2a-Fc was collected, concentrated by ultrafiltration (Ultrafree-15 centrifugal Filter Device, Millipore, Bedford, MA), and added to transfectants expressing plexins or EFN-4. The concentration of semaphorins was 25 nm. After incubation at 37° for 60 min, the cultures were washed with fresh culture medium, fixed with 4% paraformaldehyde overnight at 4°, and rinsed with TBST [10 mm Tris–Cl (pH 7.4), 150 mm NaCl, 1% Tween 20]. The cultures were then reacted with goat anti-human Ig-Fc conjugated with alkaline phosphatase (AP) (20 μg/ml, Cappel) in TBST containing skim milk (50 mg/ml) at room temperature for 1 hr. After washing with TBST, the cultures were stained in NBT/BCIP (4-nitroblue tetrazolium/5-bromo-4-chloro-3-indolyl-phosphate) solution (Boehringer) at room temperature for 5–30 min or at 4° overnight.

To confirm the expression of wild-type and mutant plexins on the cell surface, intact transfected cells were treated with anti-*myc* antibody (9E10; Evan *et al.* 1985). Then, the cells were fixed, reacted with AP-conjugated anti-mouse Ig (Zymed) and stained similarly. Expression of EFN-4 on the cell surface was confirmed with anti-EFN-4 antibodies (Chin-Sang *et al.* 2002). Immunoblot analysis was carried out as described (Fujii *et al.* 2002).

Generation of *plx-1* transgenic lines: To express PLX-1 and deletion derivatives in ray precursor cells, we used the *lin-32* promoter (*lin-32*p) (Portman and Emmons 2000). A 3.3-kb genomic sequence immediately 5′ to the *lin-32* initiation codon (T14F9 nt 25,069–28,359) was PCR amplified and subcloned into the *Pst*I site in pPD49.26. cDNAs flanked by synthetic *Kpn*I sites at both 5′- and 3′-ends were inserted into the multiple cloning site II to generate transgenes under the

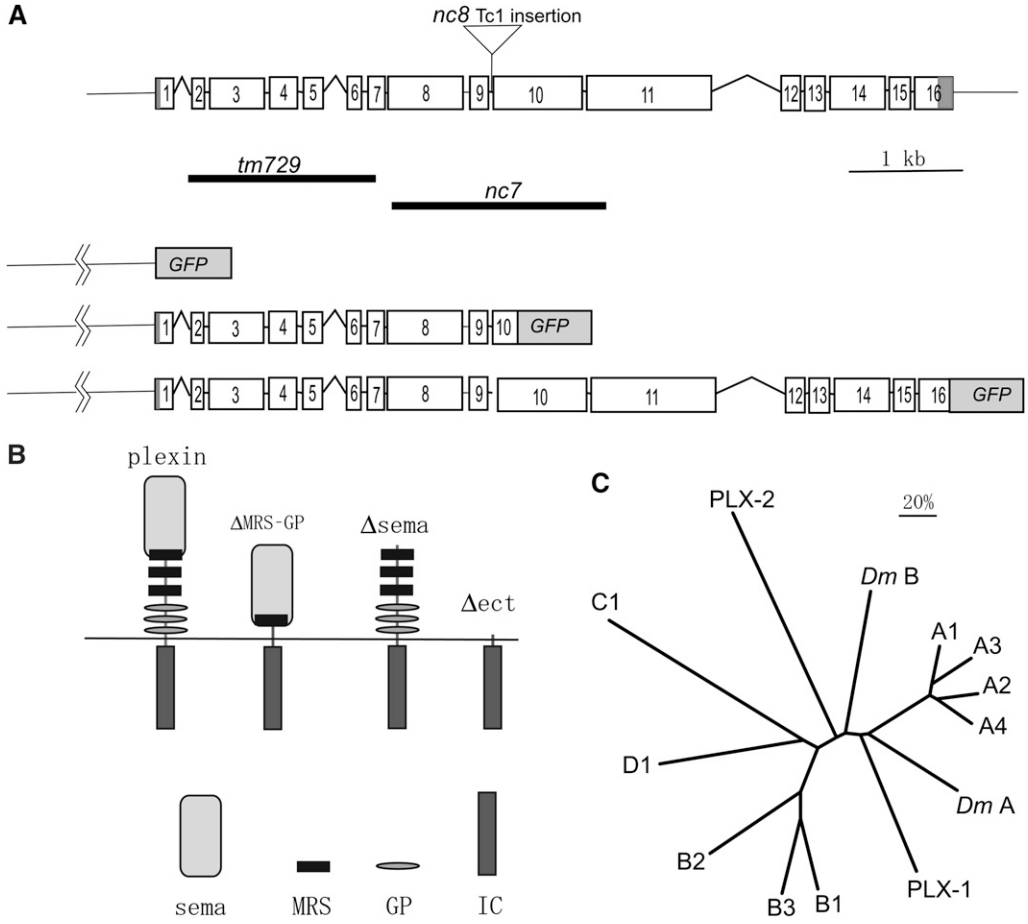

FIGURE 1.—Structure of the *plx-2* gene and PLX-2 protein. (A) Genomic structure of the *plx-2* gene, location of deletions, and structure of the translational fusion construct (PLX-2::EGFP) used in the expression analysis. (B) Structures of wild-type and mutant plexin molecules (ΔMRS-GP, Δsema, Δect) used in this study. The sema domain (sema), MRS, GP. and intracellular (IC) regions are shown below. (C) A phylogenetic tree of *C. elegans* (PLX-1, PLX-2), Drosophila [Plex A (*Dm*A), Plex B (*Dm*B)], and vertebrate plexins. The entire sequences of plexins were compared using the phylogeny analysis program PROPARS, as implemented in Joe Felsenstein's program PHYLIP 3.6 (http://evolution.genetics.washington.edu/phylip.html). The vertebrate plexin sequences used are from humans except plexin A4 (mouse).

control of *lin-32*p. The *lin-32*p*::plx-1* cDNA (0.1 mg/ml) or *lin-32*p*::plx-1ΔMRS-GP* cDNA (0.1 mg/ml) was mixed with pRF4 (0.5 mg/ml) containing *rol-6(su1006)* and injected into wild-type hermaphrodites to establish the stable extrachromosomal array, *ncEx967* and *ncEx961*, respectively.

RESULTS

***C.elegans* PLX-2 is a divergent plexin that binds the class 2 semaphorin MAB-20:** *plx-2* corresponds to transcription unit K04B12.1, located at the right end of chromosome II (Figure 1A). The predicted PLX-2 protein is composed of 1766 amino acid residues and contains all the hallmark features of plexins: a sema domain (amino acid residues 50–479), three MRSs (residues 447–479, 578–616, and 708–747), three GP repeats (residues 750–776, 847–877, and 927–956), a transmembrane region (1115–1141), and an intracellular region (1142–1766) (Figure1B).

The intracellular region of PLX-2, like that of other plexins, contains two regions of sequence conservation that together define the plexin-specific "sex-plex" (SP) domains. Overall, the PLX-2 intracellular region is highly diverged relative to those of other plexins (*e.g.*, 32% identity to Drosophila PlexB and 31% identity to mammalian Plexin Ds, whereas the *C. elegans* PLX-1 intracellular domain is 50% identical to mammalian PlexAs). Within the SP domain, PLX-2 contains a motif (**FTLADYG**, 1457–1463) similar to that in Drosophila PlexB (N**TLAHYG**, 1722–1728) reported to be necessary for binding to Rac (Hu *et al.* 2001). PLX-2 also contains two arginine residues (R1303, R1607) corresponding to the invariant catalytic residues of Ras GTPase-activating protein (Rohm *et al.* 2000). On the other hand, the PLX-2 intracellular domain does not appear to contain other motifs found in plexins, such as the putative Cdc42/Rac-interactive-binding-like motif described in human Plexin B1 (Vikis *et al.* 2000), the segment in Drosophila PlexB (1617–1827) necessary for binding to Rho (Hu *et al.* 2001), or the carboxyl-terminal PSD-95/Dlg/ZO-1 (PDZ) domain-binding motif, through which mammalian Plexin-B1 interacts with PDZ-RhoGEF/leukemia-associated Rho GEF (LARG) (Swiercz *et al.* 2002).

Plexins were originally classified into four subfamilies, A–D (Tamagnone *et al.* 1999). A more recent analysis based on the sequences of sema domains has classified plexins into two main groups, the Plexin A subfamily and the B/C/D subfamilies (Gherardi *et al.* 2004). Whereas *C. elegans* PLX-1 consistently clusters with the Plexin A subfamily, PLX-2 appears to be a divergent member of the B/C/D group and could not be assigned to any one of these subfamilies (Figure 1C).

We tested the physical interaction of PLX-2 with *C. elegans* semaphorins *in vitro* using cultured mammalian cells. We expressed the ectodomains of SMP-1/Ce-Sema-1a tagged with the Fc region of human IgG and alkaline phosphatase (Ce-Sema-1a-ΔC-Fc-AP) or MAB-20/Ce-Sema-2a tagged with Fc (Ce-Sema-2a-Fc) in HEK293T cells, and the culture supernatants were added to cells transfected with full-length PLX-2. Ce-Sema-2a-Fc bound to HEK cells expressing PLX-2, but Ce-Sema-1a-ΔC-Fc-AP did not (Figure 2, B and C). We conclude that PLX-2 specifically binds MAB-20.

***plx-2* deletion mutations do not cause overt morphogenetic abnormalities:** To analyze the function of *plx-2*, we generated two deletion mutations, *nc7* and *tm729*. *plx-2(nc7)*, generated by transposon-mediated mutagenesis, is a deletion with breakpoints in exon 8 and exon 11 and is predicted to cause an in-frame deletion of residues D493–Q1067, corresponding to the second and third MRS and the GP-rich repeats (Figure 1B). *plx-2(tm729)*, generated by chemical mutagenesis, is a deletion with breakpoints in intron 1 and exon 7, a region encoding the sema domain. The predicted structure of the message suggests that *tm729* is a molecular null; if exon 1 is spliced to exon 8, the reading frame would terminate within exon 8 due to a frameshift.

Animals homozygous for *nc7* or *tm729* were healthy, viable, and fertile. Their movements appeared normal, and analysis of neuronal morphology using a pan-neuronal marker failed to reveal defects in the nervous system (not shown). Over 99% of *nc7* and *tm729* embryos hatched and reached adulthood ($n = 1074$ for *nc7*, and $n = 878$ for *tm729*). Almost all *nc7* and *tm729* larvae were morphologically normal (not shown), and the rays in the adult male tail were normal (Table 1, Figure 5A). These observations are in stark contrast to the highly penetrant embryonic and larval lethality and male tail-ray fusion defects of *mab-20* mutants (Baird *et al.* 1991; Roy *et al.* 2000).

The dramatic phenotypic difference between *plx-2* and *mab-20* mutants might indicate that *plx-2* mutations do not eliminate PLX-2 function, although this is not plausible, at least for *tm729*, whose putative product should lack function. Alternatively, loss of PLX-2 function by itself may not lead to phenotypes similar to *mab-20* mutants. Using different alleles of *plx-2*, a previous study has suggested the same possibility (Ikegami *et al.* 2004). To further examine this, we tried to reduce the function of PLX-2 by soaking mediated RNA interference (sRNAi) in the RNAi hypersensitive mutant *rrf-3 (pk1426)* (Simmer *et al.* 2002). sRNAi of *mab-20* partly phenocopied the ray fusions of *mab-20* mutants (Table 1), and sRNAi of *plx-1* and double sRNAi of *smp-1* and *smp-2* caused ray 1 displacement comparable to that caused by genetic null mutations (not shown), showing that sRNAi is effective during ray morphogenesis. RNAi of *plx-2* did not lead to ray defects (Table 1) or to embryonic lethality (data not shown). On the basis of the

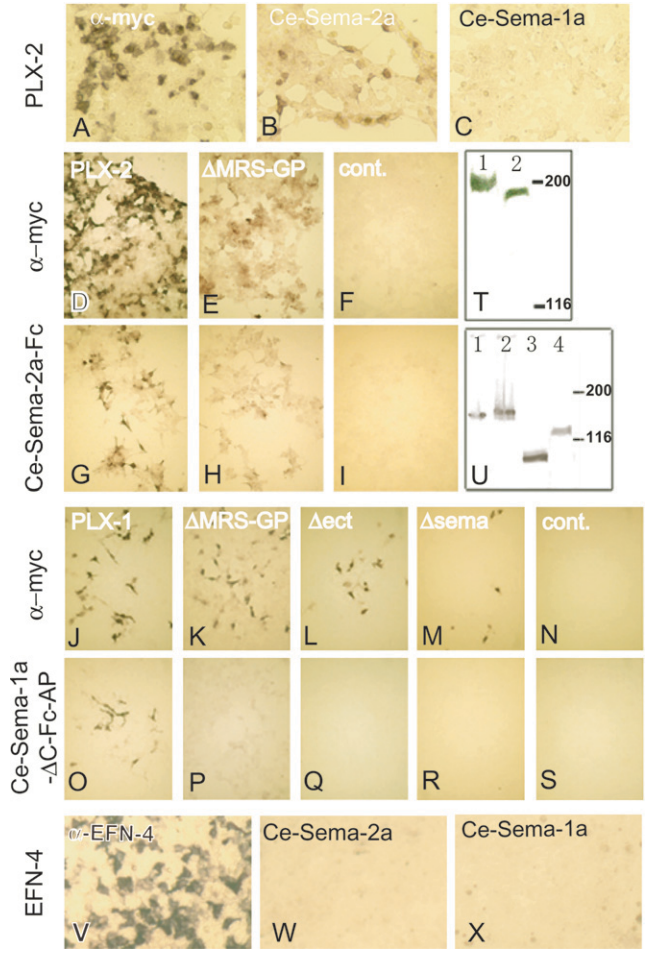

Figure 2.—*C. elegans* semaphorin 2A/MAB-20 specifically binds PLX-2. (A–C) PLX-2 bound to Ce-Sema-2a but not to Ce-Sema-1a. HEK293T cells expressing PLX-2 were reacted with Ce-Sema-2a-Fc (B) and Ce-Sema-1a-ΔC-Fc-AP (C). (D–I) PLX-2ΔMRS-GP bound to Ce-Sema-2a. HEK293T cells expressing PLX-2 (G), PLX-2ΔMRS-GP (H), and HEK293T cells transfected with the vector pCAGGS (I) were reacted with Ce-Sema-2a-Fc. (J–S) Both the sema domain and the region containing MRS–GP were required for PLX-1 to bind to Ce-Sema-1a-ΔC-Fc-AP. HEK293T cells expressing PLX-1 (O), PLX-1ΔMRS-GP (P), PLX-1Δect (Q), and PLX-1Δsema (R) and HEK293T cells transfected with pCAGGS (S) were reacted with Ce-Sema-1a-ΔC-Fc-AP. The wild-type and mutant plexins were *myc* tagged, and their expressions on the cell surface were confirmed by reacting intact transfected cells with an anti-*myc* antibody. HEK293T cells expressing PLX-2 (A and D), PLX-2ΔMRS-GP (E), PLX-1 (J), PLX-1ΔMRS-GP (K), PLX-1Δect (L), and PLX-1Δsema (M) and HEK293T cells transfected with pCAGGS (F and N) were reacted with the anti-*myc* antibody. (T and U) Expression of full-length and mutant plexins in HEK293T cells. (T) We detected immunoreactive bands of 220 and 192 kDa for *myc*-PLX-1 (lane 1) and *myc*-PLX-2 (lane 2), respectively. (U) Expression of PLX-1ΔMRS-GP, PLX-1Δsema, PLX-1Δect, and PLX-2ΔMRS-GP (lanes 1–4). We detected bands corresponding to the predicted sizes of 157, 163, 96, and 133 kDa with anti-*myc* staining. (V–X) HEK293T cells expressing EFN-4 were stained with an anti-EFN-4 antibody (V), Ce-Sema-2a-Fc (W), and Ce-Sema-1a-ΔC-Fc-AP (X). Neither MAB-20 nor SMP-1 bound to EFN-4 directly.

TABLE 1

Male tail-ray fusions in *plx-2*, *mab-20*, and *efn-4* mutant combinations

Genotype	Fusion of individual rays (%)						Fusion groups		*n*
	Ray 1	Ray 2	Ray 3	Ray 4	Ray 5	Ray 6	Three or more rays	Four or more rays	
Control (*him-5*)	0	0	0	0	0	0	0	0	313
1. Lack of ray fusion defects in *plx-2* loss of function									
plx-2(tm729)	0	0	0	0	0	0	0	0	198
plx-2(nc7)	2	2	0	0	0	0	0	0	152
plx-2(RNAi)	0	1	1	0	0	0	0	0	68
2. *plx-2* enhances *mab-20* hypomorphs									
mab-20(bx61ts)	12	18	48	46	0	1	3	0	217
bx61 tm729	12	22	*74*	*69*	0	1	9	0	214
bx61 nc7	13	24	*69*	*61*	0	1	5	0	215
mab-20(bx24)	43	69	82	79	0	25	33	8	237
bx24 tm729	76	85	95	93	0	*50*	*60*	*17*	233
bx24 nc7	56	86	92	92	1	*49*	*63*	*27*	242
3. *plx-2* does not enhance *mab-20* null									
mab-20(e574)	87	98	95	98	2	80	92	57	109
ev574 tm729	97	100	94	91	4	58	83	55	107
ev574 nc7	91	96	91	86	6	63	82	51	117
4. *plx-2* enhances *efn-4* null									
efn-4(bx80)	37	79	97	90	6	50	67	31	107
bx80 tm729	92	98	94	94	2	*68*	*85*	*56*	126
bx80 nc7	89	94	94	84	10	*75*	*91*	*57*	129
5. *efn-4* does not enhance *mab-20* or *mab-20; plx-2*									
bx61 bx80	82	96	97	92	4	52	80	44	100
bx24 bx80	87	99	98	91	1	56	85	48	100
ev574 bx80	95	100	96	99	4	79	87	51	100
bx61 tm729 bx80	91	100	99	91	3	69	89	40	100
bx24 tm729 bx80	95	100	98	95	7	63	86	49	100
ev574 tm729 bx80	91	98	95	98	5	71	78	55	100

We scored the percentage of male tail sides in which the indicated rays had fused, and the percentage of sides containing at least three or at least four rays within a single fused group. All strains contained *him-5(e1490)* and were maintained at 20°. The *mab-20* RNAi experiment is in the *rrf-3* genetic background. We did not score ray fusions involving rays 7–9. *n*, number of sides. 1: Loss of *plx-2* function by mutation or by soaking RNAi does not cause significant ray fusion defects. 2: *plx-2* mutations enhance weak ray fusion defects of *mab-20* hypomorphic alleles. *bx61* at the semipermissive temperature of 20° causes partially penetrant fusions of rays 3 and 4 that are significantly enhanced in *plx-2* mutant backgrounds. *bx24* causes partially penetrant fusions of ray 6 that are enhanced in *plx-2* double mutants. Percentages in italics are significantly different from the matched *plx-2(+)* control ($P < 0.01$, Fisher's exact test). 3: *plx-2* does not enhance *mab-20(ev574)*. For ray 6 fusion, *plx-2* may slightly suppress *ev574* phenotypes. 4: *plx-2* enhances *efn-4(bx80)* for ray 6 fusion and fusion groups. 5: *efn-4* does not enhance *mab-20*. Penetrance of ray fusions in double and triple mutants is not enhanced beyond that of the strongest single mutant.

absence of a phenotype in mutant alleles, including deletion alleles, and negative results with RNAi, we conclude that loss of *plx-2* function alone does not cause overt defects in morphogenesis resembling those of *mab-20* mutants.

Genetic interactions of *plx-2*, *mab-20*, and *efn-4* mutations: To address whether PLX-2 has a cryptic role in MAB-20 signaling, we constructed double mutants between *plx-2* and three *mab-20* alleles: the hypomorphic alleles *bx61* and *bx24* and the predicted null mutation *ev574* (Roy *et al.* 2000). *mab-20(bx61)* is a temperature-sensitive allele caused by a missense mutation and causes weak ray fusion defects at 20°. *mab-20(bx24)* is a hypomorphic allele of medium strength that contains an out-of-frame tandem duplication. We refer to *bx61* and *bx24* collectively as weak *mab-20* alleles. *mab-20(ev574)* is a deletion that includes the initiator methionine. *ev574* is predicted to be a molecular null and causes the most

severe morphogenetic defects among the three *mab-20* alleles.

First we examined whether *plx-2* mutations affect the lethality of *mab-20* mutants using double-mutant analysis. The hypomorphic mutation *mab-20(bx24)* causes incompletely penetrant (9%) embryonic lethality (Figure 3A). Both *plx-2(tm729)* and *plx-2(nc7)* significantly enhanced the penetrance of the embryonic lethality of *bx24*: 16 and 17% of embryos failed to hatch for *bx24; tm729* and for *bx24; nc7*, respectively. *plx-2(tm729)* also enhanced the penetrance of embryonic lethality of *bx61*. In contrast, neither *plx-2(tm729)* nor *plx-2(nc7)* enhanced the embryonic lethality of the null allele *mab-20(ev574)*: 22 and 21% of embryos failed to hatch for *ev574; tm729* and for *ev574; nc7*, respectively. We found similar trends in larval lethality (Figure 3B). As *plx-2* mutations enhanced the embryonic phenotypes of weak *mab-20* alleles but not of *mab-20* null alleles, we conclude that PLX-2 has a cryptic role in MAB-20 signaling revealed when MAB-20 function is compromised.

The dramatic difference in penetrance between *plx-2* and *mab-20* null mutants strongly argues that MAB-20 has functions independent of PLX-2. As the other plexin, PLX-1, does not appear to function in MAB-20 signaling (Fujii *et al.* 2002), we tested the role of another potential component of MAB-20 pathways, the ephrin EFN-4. First we examined the genetic interaction between *plx-2* and *efn-4* mutants. *efn-4(bx80)* is a putative null allele (Chin-Sang *et al.* 2002). Both *plx-2(nc7)* and *plx-2(tm729)* significantly enhanced the embryonic and larval lethality of *efn-4(bx80)* beyond that expected for additivity of phenotypes: 10% of *bx80* embryos failed to hatch, whereas 20% of *tm729; bx80* or 20% of *nc7; bx80* failed to hatch (Figure 3A; $P < 0.05$ by ANOVA). *plx-2* mutations also enhanced the larval lethality of *efn-4(bx80)* (Figure 3B) to a level similar to that of *mab-20* null mutants. The enhancement of *efn-4* null phenotypes by *plx-2* suggests that PLX-2 and EFN-4 act in parallel and have partly redundant roles in morphogenesis.

We previously reported that certain *mab-20; efn-4* double mutants display subadditive interactions in embryonic and larval lethality (Chin-Sang *et al.* 2002). We confirmed and extended this finding using null mutations in both genes. Interestingly, we found that *efn-4 (bx80)* partly suppressed the penetrance of the embryonic lethality of *mab-20(ev574)* (Figure 3A); the double mutants displayed an intermediate level of lethality compared to the single mutants. This partial genetic suppression suggests that MAB-20 and EFN-4, while having similar roles in some situations may antagonize in other contexts (see below). Although the *mab-20* null allele *ev574* was consistently suppressed by *efn-4*, the weak *mab-20* alleles, *bx24* and *bx61*, enhanced the embryonic lethality of *efn-4* null mutants; the penetrance of embryonic defects in these double mutants did not exceed that of *mab-20(ev574)*. These results from homozygous double mutants are reminiscent of the finding that *bx61*, but not *ev574*, displays dosage-sensitive interactions with *efn-4(bx80)* (Ikegami *et al.* 2004).

The overlap in *efn-4* and *mab-20* phenotypes and the enhancement of *efn-4* by weak *mab-20* alleles suggest that MAB-20 positively regulates EFN-4. To account for the partial suppression of *mab-20(ev574)* by *efn-4*, we propose that EFN-4 is partly activated by MAB-20/PLX-2 signals, but that MAB-20 is not essential for all PLX-2 activity. Studies of vertebrate plexins have led to the model that plexins are autoinhibited until they interact with semaphorin ligand; a plexin therefore might have a low level of activity in the absence of ligand. MAB-20 can be thought of as both positively and negatively regulating PLX-2. We hypothesize that, in the wild-type, MAB-20 binds PLX-2 and this promotes EFN-4 function. In *mab-20* weak mutants, mutant MAB-20 products that bind PLX-2 are expressed, and these mutant complexes retain a residual ability to activate EFN-4, and thus mutation of *efn-4* does not suppress *mab-20* weak alleles. In contrast, in the complete absence of MAB-20, PLX-2 is constitutively active and can increase EFN-4 function. Elimination of EFN-4 therefore partly alleviates the *mab-20* null phenotype. This model predicts that lack of *plx-2* should block the suppression of *mab-20(ev574)* by *efn-4 (bx80)*, and we find that this is the case: triple null mutants of genotype *mab-20(ev574); plx-2(tm729); efn-4 (bx80)* resemble *mab-20(ev574)* and not *mab-20; efn-4* in overall penetrance (Figure 3). The significant differences in penetrance between *mab-20; efn-4* and *mab-20; plx-2; efn-4* strains ($P < 0.05$, ANOVA) imply that PLX-2 has some activity in the absence of either MAB-20 or EFN-4. As MAB-20 also positively regulates PLX-2, elimination of PLX-2 does not itself suppress the *mab-20* null phenotype.

PLX-2 has a minor role in embryonic ventral neuroblast movement and acts redundantly with EFN-4 in later epidermal morphogenesis: Both *mab-20* and *efn-4* mutants display incompletely penetrant defects in embryonic epidermal morphogenesis. Defective epidermal morphogenesis can result from cell-autonomous defects in the epidermal epithelium or from defective formation of the underlying substrate for enclosure, which itself is formed by coordinated migrations of ventral neuroblasts (VNBs) at the end of gastrulation (Chisholm and Hardin 2005). We previously reported that during embryogenesis both *efn-4* and *mab-20* mutants display delayed VNB migrations (Chin-Sang *et al.* 2002; Hudson *et al.* 2006). To understand the role of *plx-2* in the MAB-20 and EFN-4 pathways in embryogenesis, we quantitatively analyzed VNB migrations and morphogenetic movements in single, double, and triple null mutants using time-lapse microscopy (Figure 4, A and B).

Approximately 10% of *efn-4(bx80)* mutants arrested at the epidermal enclosure stage of embryogenesis, a phenotype denoted class I or II, depending on the degree of enclosure reached (Chin-Sang *et al.* 2002). In most *efn-4* mutants, VNB migrations are slightly delayed and the

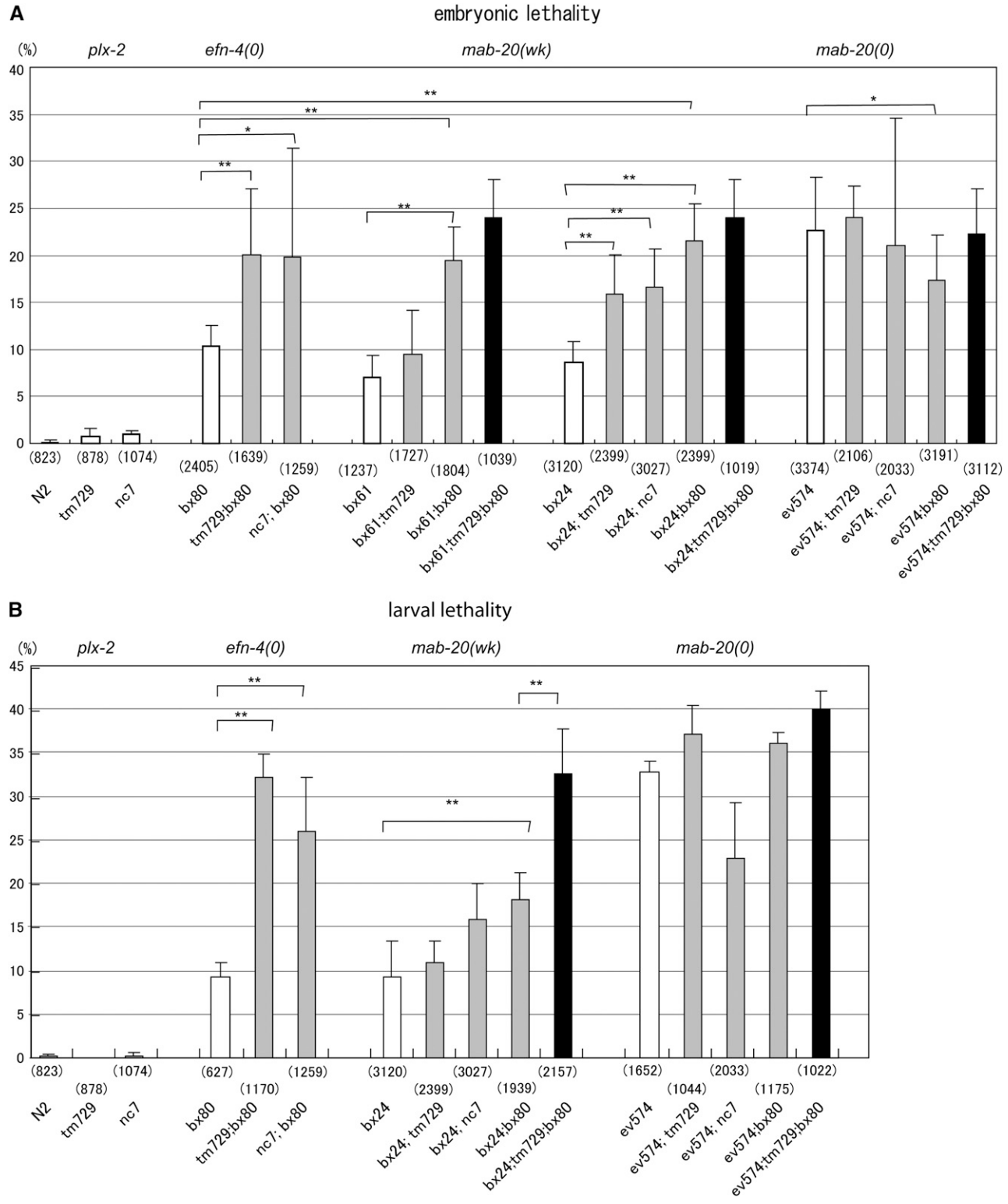

FIGURE 3.—Penetrance of embryonic and larval lethality and adult epidermal phenotypes in *plx-2*, *mab-20*, and *efn-4* mutant combinations. (A) Penetrance of embryonic lethality in *plx-2*, *mab-20*, and *efn-4* single mutants (open bars); *mab-20; plx-2*, *plx-2; efn-4*, and *mab-20; efn-4* double mutants (shaded bars), and the *mab-20; plx-2; efn-4* triple mutant (solid bars). Error bars indicate the SEM. *plx-2* mutants rarely exhibit embryonic lethality. The *plx-2* mutations significantly enhanced the penetrance of the embryonic lethality of the *mab-20* weak alleles *(wk)*, *bx24* and *bx61*, and the *efn-4* null allele, *bx80*, but not that of the *mab-20* null (*0*) allele, *ev574*. *bx80* also enhanced the penetrance of embryonic lethality of the *mab-20* weak alleles, but suppressed that of the *mab-20* null allele slightly. Differences in penetrance were compared using ANOVA and are shown only for the relevant pair being compared. $*P < 0.05$; $**P < 0.001$. (B) Penetrance of larval lethality in *plx-2*, *mab-20*, and *efn-4* mutant combinations.

(*Continued*)

epidermis encloses. In contrast, *mab-20* mutants display more variable VNB migration defects that rarely result in class I/II arrest. Embryonic lethality in *mab-20* null mutants is predominantly due to rupture of the epidermis in the elongation stage of embryogenesis (the class III terminal phenotype; Figure 5A), suggesting MAB-20 becomes more critical in later epidermal morphogenesis (Roy *et al.* 2000). VNB migrations of *mab-20; efn-4* double null mutants were not significantly different from those of *efn-4* single mutants (Figure 4B). *mab-20; efn-4* double mutants displayed enclosure stage arrest (class I/II) at a frequency similar to that of *efn-4* single mutants (Figure 5C). Thus, although *mab-20* null mutants display delayed VNB migrations, they do not enhance the VNB migration or enclosure defects of *efn-4* mutants, consistent with MAB-20 and EFN-4 acting in a common process regulating VNB movement. In contrast, *efn-4; mab-20* double mutants displayed a reduced level of class III arrest compared to *mab-20* mutants, accounting for the partial suppression of embryonic lethality (Figure 5C). These observations suggest that the antagonism of MAB-20 and EFN-4 may be specific to later embryonic development.

We examined the embryonic development of *plx-2* mutants. Ventral cleft closure duration in *plx-2* mutants was slightly prolonged relative to the wild type (64 ± 15 min in *tm729 vs.* 55 ± 15 min in the wild type; $P = 0.04$ by *t*-test). *plx-2* mutants did not show penetrant defects in epidermal enclosure or in later embryogenesis. Unlike *tm729*, the in-frame deletion allele *plx-2(nc7)* did not affect the duration of cleft closure; in *nc7* mutants, the onset of cleft closure was earlier than in the wild type (not shown). *plx-2(tm729)* did not significantly enhance the VNB migration defects of either *efn-4*, *mab-20* or *mab-20; efn-4* double mutants (Figure 4B).

These findings suggested that PLX-2 plays a relatively minor role in VNB movement compared to that of EFN-4 or MAB-20. To test whether a cryptic role for PLX-2 in VNB movement would be revealed in a more sensitized background, we constructed double mutants between *plx-2* and *kal-1*, a gene required for normal VNB migration (Hudson *et al.* 2006). *kal-1* null mutants display delayed VNB migrations that do not typically result in embryonic lethality, but which strongly enhance VNB migration defects of *efn-4* or *mab-20* null alleles. We found that *plx-2(tm729)* did not significantly enhance *kal-1* VNB migration or other morphogenetic defects. *kal-1(gb503); plx-2(tm729)* double mutants displayed a cleft duration of 74.4 min [$n = 21$; $P = 0.1$ compared to *kal-1(gb503)* alone] and <1% embryonic lethality, consistent with a relatively minor role for PLX-2 in ventral neuroblast movements.

As *plx-2* mutations significantly enhanced the total embryonic lethality of *efn-4* mutants, these findings suggest that PLX-2 and EFN-4 have redundant roles in later embryogenesis. The enhancement of *efn-4* embryonic lethality can be largely accounted for by the higher rates of elongation-stage rupture compared to *efn-4* alone (Figure 5C; $P < 0.05$, Fisher's exact test). The frequency of late embryonic epidermal ruptures in *plx-2; efn-4* strains (13.8%) was not further enhanced in the *mab-20; plx-2; efn-4* triple mutant (14.3%), consistent with EFN-4 and PLX-2 acting redundantly in the MAB-20-dependent process that promotes later embryonic epidermal development.

PLX-2 is expressed in embryonic neuronal and epidermal cells and is partly overlapping with EFN-4 in the posterior epidermis: To address whether EFN-4 and PLX-2 might function in the same cells in MAB-20 signaling, we compared in detail the embryonic expression patterns of PLX-2 transcriptional and translational reporters and a functional EFN-4::GFP reporter (*juIs109*). In early embryos, EFN-4::GFP is widely expressed in ventral neuroblasts prior to epidermal enclosure (Chin-Sang *et al.* 2002). In contrast, PLX-2 reporters were expressed in a much smaller number of ventral neuroblasts (Figure 6A), consistent with our embryological data showing that EFN-4 acts independently of PLX-2 in VNB movement. Following epidermal enclosure, PLX-2::GFP reporters were expressed in neurons and in a subset of posterior lateral and ventral epidermal cells; we identified these as the lateral cell QV5 and the ventral epidermal cells P9–12 (Figure 6, B–D). In addition to its widespread neuronal expression, we find that EFN-4::GFP is also expressed in anterior and posterior epidermal cells, including the lateral epidermal cells H0 and QV5, the leading ventral epidermal cells of the anterior, and the posterior three pairs of ventral epidermal cells (P7–12) (Figure 6, E–H). The overlap in PLX-2 and EFN-4 expression in the posterior embryonic epidermis correlates with the defect in posterior ventral epidermal integrity of *plx-2; efn-4* double mutants and suggests that in this process EFN-4 and PLX-2 could act in the same or adjacent cells to mediate a MAB-20 cell rearrangement signal.

PLX-2 and EFN-4 promote MAB-20-dependent sorting of ray cells: In both *mab-20* and *efn-4* mutants, male sensory rays become aberrantly fused, a phenotype suggestive of a failure of cell sorting or repulsion between the component cells of a ray. Neither *plx-2(nc7)* nor *plx-2 (tm729)* caused overtly abnormal ray development as single mutants (Table 1, although see below for Rn.p defects). In larval male tails, PLX-2 reporters were strongly expressed in neurons and muscles and weakly expressed

plx-2 mutants do not exhibit larval lethality. *plx-2* (*tm729)* enhances the larval lethality of *efn-4(bx80)* null mutants, but not that of the *mab-20(ev574)* null allele. *efn-4(bx80)* does not significantly enhance the larval lethality of *mab-20(ev574)*. The numbers of animals examined are shown in parentheses below bars.

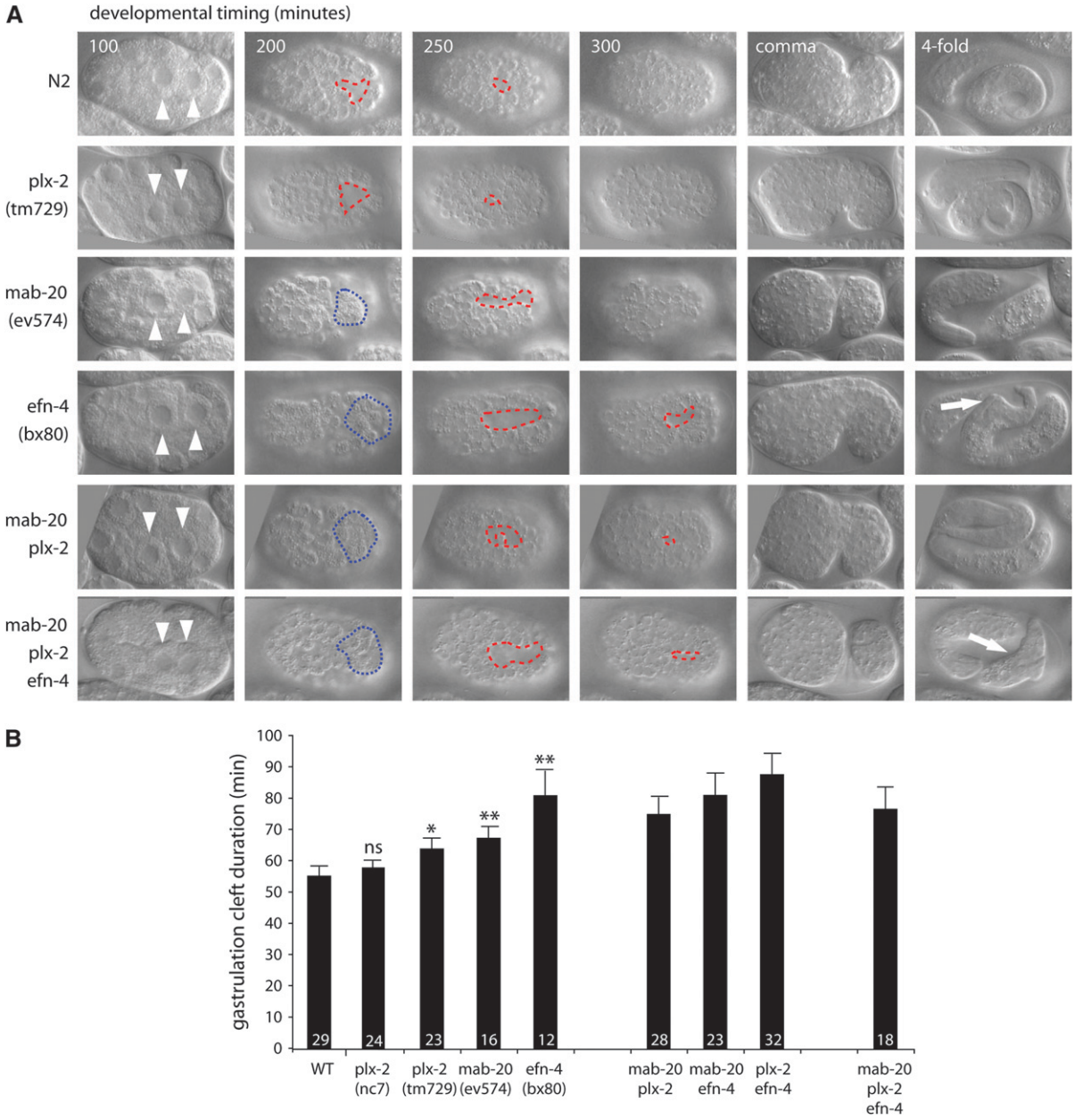

FIGURE 4.—PLX-2 plays a minor role in ventral neuroblast migration. (A) DIC micrographs of *C. elegans* embryogenesis. Gastrulation commences ~100 min after the first cell division with ingression of the Ea and Ep gut precursors (arrowheads). At 200 min, a transient cleft is formed on the ventral surface of the embryo (red dashed line), caused by ingression of mesodermal cells. The cleft is closed by short-range lateral movements of VNBs, which generate a substrate for the epidermis during enclosure. *plx-2* mutants show a small but significant delay in cleft closure. *mab-20* mutants show some disorganization during gastrulation, which leads to an apparent delay in cleft opening (the blue dotted line illustrates D granddaughters remaining on the ventral surface of the embryo) and a significant ($P < 0.01$) delay in cleft closure. *efn-4* mutants show similar but stronger defects, with D granddaughter ingression delayed by ~25 min. Closure of the cleft is delayed further still, with ~10% of embryos failing to close the cleft at ventral enclosure, resulting in embryonic rupture and death. *mab-20; plx-2* double mutants are similar to *efn-4* single mutants, whereas *mab-20; plx-2; efn-4* triple mutants show delayed cleft opening, but earlier cleft closure. *mab-20; efn-4* double mutants resemble the triple mutant in phenotype (not shown). Variably penetrant morphological defects in the tail are apparent in *mab-20* and *efn-4* mutant combinations at the fourfold stage (arrows). (B) Gastrulation cleft duration in *mab-20, plx-2* and *efn-4* strains. Each single mutant shows significantly longer cleft duration compared to wild type ($P < 0.05$ for *plx-2* and <0.01 for *mab-20* and *efn-4*). Double and triple mutants are not significantly different from the strongest single-mutant strain.

in some unidentified epidermal cells. We confirmed GFP expression in the tail seam cells and R7/8/9.p (Figure 7, D and F). However, we could not detect translational PLX-2::GFP reporters in Rn cells, or many of their descendants, suggesting that this PLX-2::GFP reporter may not reflect the complete PLX-2 expression pattern.

To test whether PLX-2 had a cryptic role in ray development comparable to the embryo, we examined double

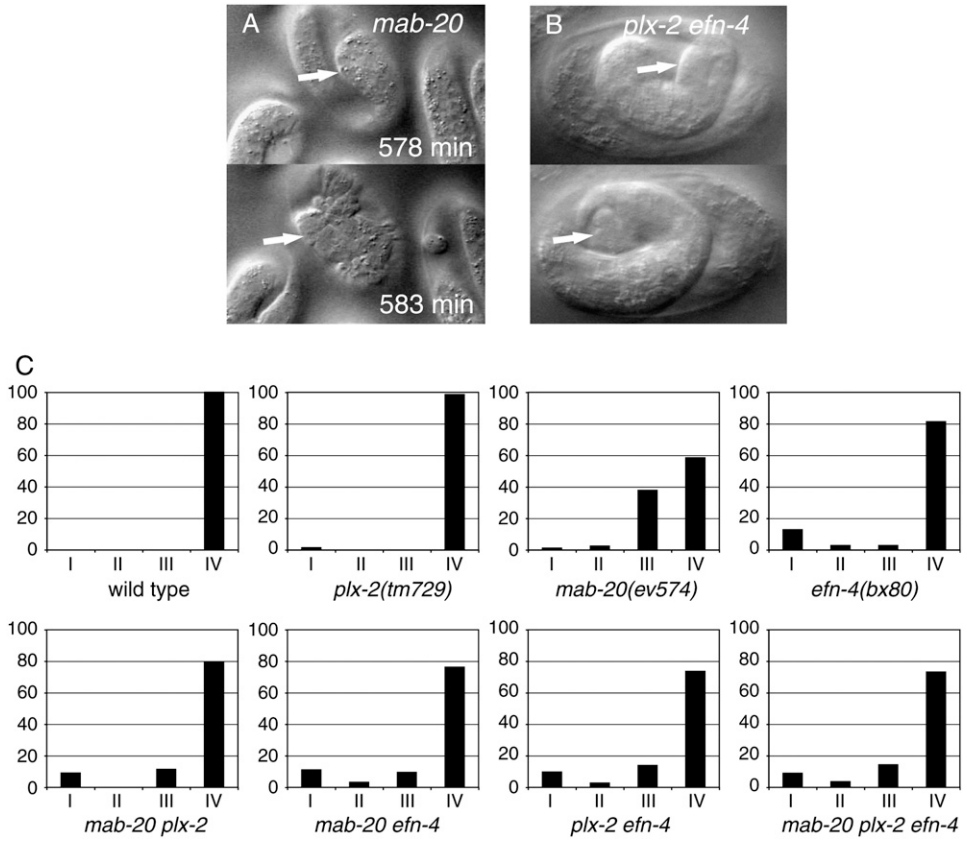

FIGURE 5.—*mab-20* late embryonic epidermal rupture is recapitulated in *plx-2; efn-4* double mutants. (A) Late embryonic rupture phenotype (class III arrest) characteristic of *mab-20* embryos. *mab-20* embryos typically enclose the epidermis at the normal time and then undergo aberrant epidermal elongation in which the posterior ventral epidermis is bulged and deformed (arrow, top) and eventually ruptures in the ventral preanal region ~4 hr after enclosure (arrow points to extruding cells, bottom). Panels in A are from a 4D movie of *mab-20(ev574)*. (B) Similar late embryonic rupture in the ventral posterior epidermis is seen in *plx-2(tm729); efn-4(bx80)* double mutants but not in the single mutants. (C) Quantitation of embryonic arrest classes. We quantified embryonic terminal phenotypes in embryos followed at 2-hr intervals using DIC microscopy ($n > 50$ for each genotype). Embryonic arrest stages were classified as follows: 1, arrest at epidermal enclosure due to failure to enclose epidermis (corresponding to 4D classes I and II); 2, rupture at two- to threefold stage of elongation; 3, rupture at three- to fourfold stage (shown in A and B); 4, development to hatched L1. Type 1 arrest (enclosure) is frequent in *efn-4* and rare in *plx-2* and *mab-20*. Type 3 arrest is rare in *plx-2* or *efn-4* single mutants but is common in *efn-4; plx-2* double mutants and is the predominant mode of embryonic arrest in *mab-20* single mutants.

and triple mutants. We found that both *plx-2* mutations significantly enhanced ray fusion defects of weak *mab-20* alleles (Table 1, section 2; Figure 7C) but not of the null mutation *mab-20(ev574)*, implying that PLX-2 promotes MAB-20 functions in ray development. Both *plx-2(nc7)* and *plx-2(tm729)* also significantly enhanced the ray fusion defects of *efn-4(bx80)* (Table 1, section 4), consistent with EFN-4 and PLX-2 acting in parallel to promote ray cell sorting. Since ray fusion reflects aberrant aggregation of ray precursor (Rn.a-derived) cell clusters, we also analyzed the arrangement of ray precursors in larval males using the apical junction marker AJM-1::GFP (Figure 7, H and I). Using this marker, we found that precursor clusters were arranged normally in *plx-2 (tm729)* larvae ($n = 50$). *plx-2(tm729)* significantly enhanced the aggregation of ray precursor clusters in *mab-20* weak alleles (Figure 7, J and N), consistent with enhancement of the ray fusion defects in the adult double mutants.

Our analysis of ray development suggests that the role of MAB-20 in preventing inappropriate cell contacts involves partly redundant functions of EFN-4 and PLX-2. However, because *mab-20(ev574)* single mutants display very highly penetrant ray fusion defects, further enhancement in a double mutant may not be easily detectable. In addition, ray precursor (Rn.a) clusters in *mab-20(ev574)* and *efn-4(bx80)* mutants were often so severely disorganized that individual clusters could not be scored. Since we found that the morphology of Rn.p epidermal cells adjacent to ray precursor clusters was often abnormal in these mutants, we used it as an alternative index of arrangement defects of tail epidermal cells. We categorized Rn.p's into five classes, ranging from wild-type morphology (class I) to most disrupted (class V) (Figure 7, K–M). Eighty-one percent of *mab-20* mutants displayed Rn.p defects, whereas 67% of *efn-4* mutants had aberrant Rn.p's. Eighty-six percent of *mab-20; efn-4* double mutants were defective, a proportion that is not significantly different from that of *mab-20* single mutants ($P = 0.25$; Figure 7O). The only difference that we could detect between *mab-20* single mutants and *mab-20; efn-4* double mutants was an increase in the proportion of class IV Rn.p morphology at the expense of class III ($P = 0.03$). We conclude that EFN-4 functions predominantly in MAB-20 signaling in Rn.p morphogenesis.

Despite having overtly normal ray morphology, *plx-2 (tm729)* males displayed low-penetrance defects in Rn.p morphology (26% type II), consistent with previous findings that *plx-2* single mutants display subtle abnormalities

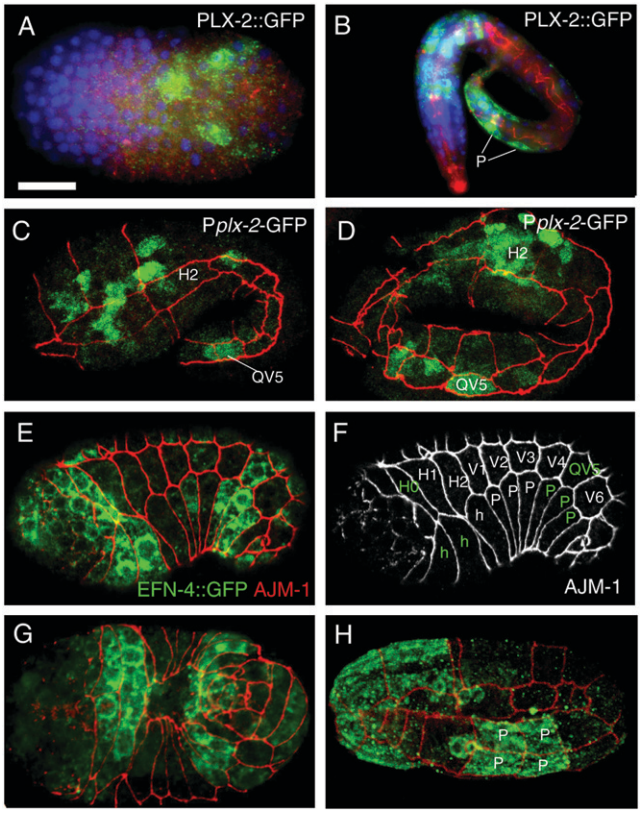

Figure 6.—Expression of PLX-2 and EFN-4 in embryonic neuronal and epidermal cells. PLX-2 and EFN-4 GFP transgene expression was detected by immunostaining with anti-GFP antibodies (green in all panels) ; samples are labeled with the anti-AJM-1 antibody MH27 (red) to visualize epidermal cell outlines. A and B are stained with DAPI (blue) to show cell nuclei. (A) A PLX-2::GFP translational fusion protein is first expressed in a small number of ventral cells prior to epidermal enclosure; these are identified as ventral neuroblasts on the basis of position. (B) In late stage embryos, PLX-2::GFP was expressed in several tail epidermal cells, including the preanal ventral epidermal cell pairs P11/12 and P9/10 (indicated as "P" with white lines). PLX-2::GFP was also expressed in numerous neurons in the head and tail. (C and D) Expression of PLX-2 in the QV5 lateral epidermal cell at the 1.5- and 2-fold stage, detected using the P*plx-2*-GFP transcriptional reporter *ncIs21*; images are projections of surface focal planes from a confocal z-stack. (E–H) EFN-4::GFP (*juIs109*) is expressed in a subset of epidermal cells during and after epidermal enclosure. During enclosure (lateral views in E and F; ventral view in G), EFN-4::GFP was detected in the lateral epidermal cells H0 and QV5, in the leading anterior epidermal cells (green "h") in the head region, and in the three posterior pairs of P cells (P7/8, 9/10, 11/12) (green P cells marked in AJM-1 channel in F). (H) At the 2-fold stage, EFN-4::GFP is seen in P9/10 and P11/12 (P, ventral view of preanal epidermis); expression also persists in the head ventral epidermis. EFN-4::GFP expression in epidermal cells persists until late embryonic stages and was not detectable in L1 larvae. Bar, 10 μm in all panels except B (20 μm).

in the shapes and positions of lateral epidermal cells (Ikegami *et al.* 2004). Loss of *plx-2* function did not significantly enhance Rn.p morphology defects in *mab-20(ev574)* mutants. *plx-2; efn-4* double mutants displayed a slight enhancement of class V defects relative to *efn-4* (32 *vs.* 22%) although this was not statistically significant. In general, our analysis of Rn.p morphology is consistent with both EFN-4 and PLX-2 functioning largely in a MAB-20-dependent pathway.

Different requirements for the MRS and GP repeats in plexin-semaphorin binding: *plx-2(nc7)* is an in-frame deletion predicted to create a mutant protein lacking only the second and third MRSs and the three GP-rich repeats. However, in several assays, *nc7* behaved similarly to the presumed null mutation *plx-2(tm729)*. To examine how the *nc7* deletion might affect PLX-2 function, we analyzed its effects on protein stability and ligand binding. First, we generated *plx-2* cDNA from RNA isolated from *nc7* animals by RT–PCR,and confirmed that *plx-2(nc7)* mutants express a mRNA with a smaller size corresponding to the *nc7* deletion (not shown). Next, we expressed PLX-2 resembling the *nc7* mutant version (PLX-2ΔMRS-GP) in HEK293T cells and found that, despite reduced cell surface expression compared to wild-type PLX-2 (Figure 2E), it was able to bind to MAB-20::Fc (Figure 2H). These results suggest that the MRS and GP domains of PLX-2 are not directly involved in MAB-20 binding but that they promote other aspects of PLX-2 synthesis or function.

To test whether the sema domain of PLX-1 is also sufficient for its interaction with a semaphorin, we generated similar deletions in the PLX-1 extracellular domain. Unexpectedly, deletion of the PLX-1 MRSs and three GP-rich regions, PLX-1ΔMRS-GP, completely abolished its ability to bind a SMP-1 fusion protein (Ce-Sema-1a-ΔC-Fc-AP; Figure 2P); deletion of the PLX-1 sema domain also abolished SMP-1 binding (Figure 2R). We tested whether the MRSs and three GP-rich regions are necessary for the proper function of PLX-1 *in vivo* by using a transgene expressing PLX-1ΔMRS-GP under the *lin-32* promoter, which drives gene expression in epidermal ray precursor cells (Portman and Emmons 2000). In *plx-1(nc37)* mutants, ray 1 is displaced anteriorly at high frequency (96%; $n = 117$), while in wild-type animals the displacement is rare (4%; $n = 121$). In *plx-1(nc37); ncEx967* animals, *lin-32* promoter-driven expression of wild-type PLX-1 rescued the displacement (35% anterior; $n = 107$), whereas expression of PLX-1ΔMRS-GP in *plx-1(nc37); ncEx961* animals did not rescue (96%; $n = 110$), consistent with abolished ability to bind SMP-1 *in vitro*. Taken together, our results suggest that PLX-1 and PLX-2 may interact differently with their respective semaphorin ligands.

As our genetic analyses indicated that EFN-4 acts in MAB-20 signaling, we also examined whether MAB-20 could physically interact with EFN-4 in cultured mammalian cells. EFN-4 was robustly expressed in HEK293T cells (Figure 2V). However, neither Ce-Sema-2a-Fc nor Ce-Sema-1a-ΔC-Fc-AP bound to HEK293T cells expressing EFN-4 (Figure 2, W and X). We conclude that EFN-4 is unlikely to interact directly with MAB-20.

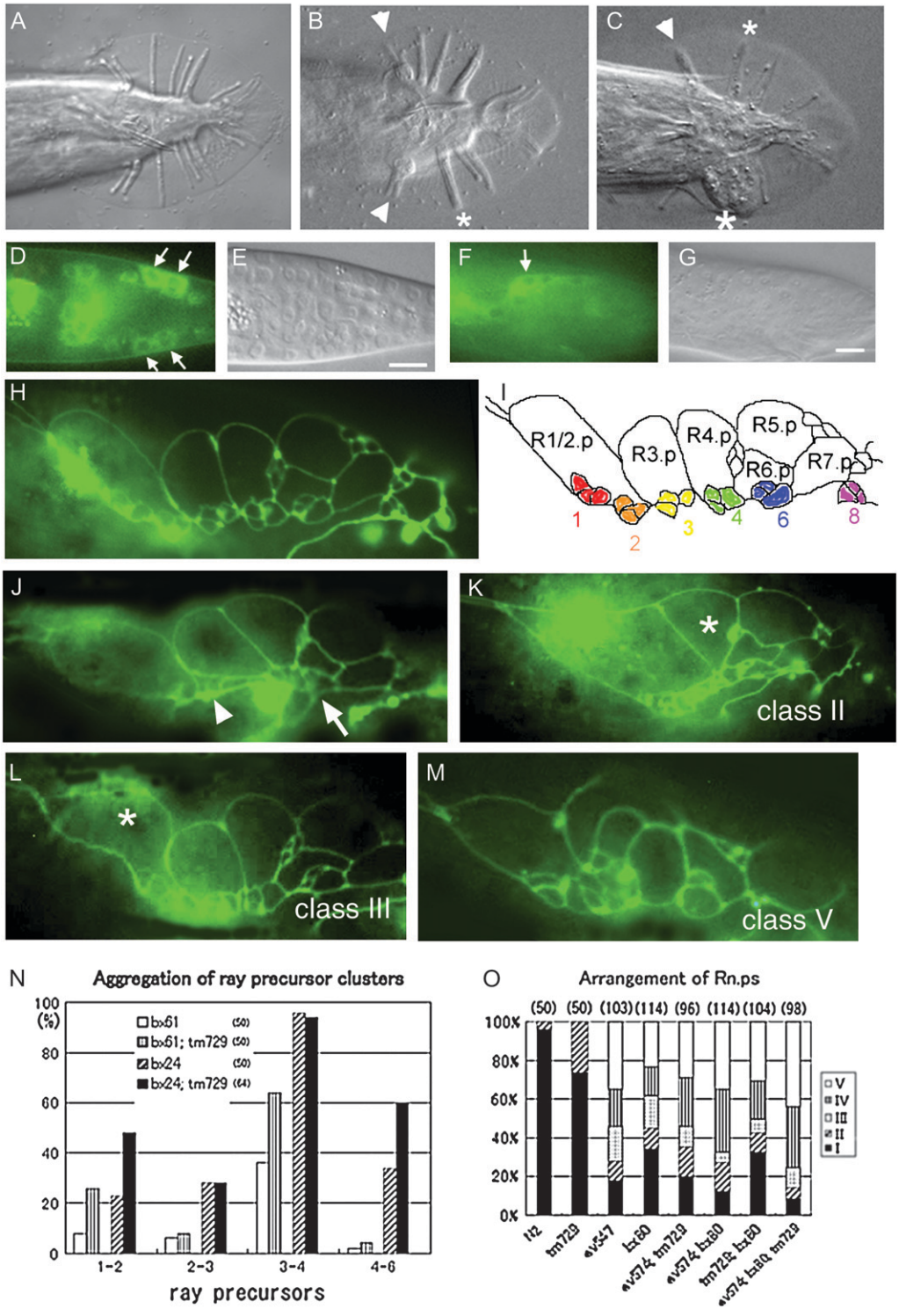

FIGURE 7.—PLX-2 and EFN-4 promote MAB-20 function in male tail-ray development. (A–C) Ventral views of adult male tails. All genotypes contain *him-5*. Anterior is to the left. (A) A *plx-2(nc7)* tail has wild-type morphology, and nine rays can be distinguished on each side. (B) In *mab-20(bx24)*, rays 1 and 2 on both sides (arrowheads) and rays 3 and 4 of the left side (an asterisk) are fused. (C) In a *mab-20(bx24); plx-2(nc7)* tail, rays 1 and 2 (an arrowhead) and rays 3 and 4 (a small asterisk) on the right side and rays 2, 3, 4, and 6 on the left side (a large asterisk) are fused. (D) The epidermal cells, R8.p and R9.p (arrows) express GFP in a third-larval-stage tail of a male carrying the partial PLX-2::GFP translational fusion. (F) Tail seam cells (SET) express GFP (arrow) in the early fourth-larval-stage male tail. The corresponding DIC images are shown in E and G, respectively. Bar, 10 μm. (H–M) Lateral view of the larval male tail to visualize epidermal cells with AJM-1::GFP. Anterior is to the left. (H) Wild-type epidermal cells and (I) a schematic to show Rn.p's and ray precursor clusters 1, 2, 3, 4, 6, and 8. (J) In a *bx61* larva, ray precursor clusters 2 and 3 (an arrowhead) and 4 and 6 (an arrow) aggregate. In animals with *mab-20* and/or *efn-4* mutations, in addition to the arrangement defects of ray precursor clusters, the morphology of Rn.p's is often abnormal. (K) R4.p (asterisk) adopted a triangular shape (class II) rather than a wild-type rectangular shape. (L) R1/2.p (asterisk) is larger or irregular compared with wild type (class III). (M) The morphology of all Rn.p's is severely affected (class V). (N) Aggregation of ray precursor clusters 1 and 2, 2 and 3, 3 and 4, and 4 and 6 was scored. *plx-2(tm729)* enhances the aggregation in weak *mab-20* alleles, whereas no aggregation is detected in any ray precursor cluster of *plx-2(tm729)* mutants ($n = 50$). (O) Frequencies of Rn.p morphological classes in *plx-2*, *mab-20*, and *efn-4* mutant combinations. The number of animals examined is shown in parentheses.

DISCUSSION

The *C. elegans* semaphorin 2a MAB-20 has pleiotropic functions in cell migration and cell adhesion in development, yet the nature of the MAB-20 signaling pathway has remained elusive. In this article we provide genetic and biochemical evidence that the plexin PLX-2 acts in a branched MAB-20 signaling pathway. We find

that *plx-2* mutations enhance multiple phenotypes of weak *mab-20* alleles, but not of a *mab-20* null allele, suggesting that *plx-2* and *mab-20* act in a common genetic pathway. We have also shown that PLX-2 binds to MAB-20, but not to another semaphorin, SMP-1. These results imply that PLX-2 is a functional receptor for MAB-20. We show that in certain contexts the atypical ephrin EFN-4 acts in parallel to PLX-2 in MAB-20-dependent processes.

PLX-2 is not the sole receptor for MAB-20/Sema 2a: PLX-2 can bind to MAB-20, consistent with a receptor–ligand relationship. However, putative *plx-2* null mutants display much weaker phenotypes when compared to *mab-20* null mutants, implying that MAB-20 can signal via a second pathway. An alternative explanation of the subtle phenotype of *plx-2* mutants compared to *mab-20* might be that PLX-2 receives both a positive signal from MAB-20 and an antagonistic signal from some other molecules, so that deletion of PLX-2 eliminates both signals and thus results in a weak phenotype compared to the *mab-20* null phenotype. However, such models predict that *plx-2* should be epistatic to *mab-20*, and this is not so. Thus, we favor the model that MAB-20 signals via a PLX-2-dependent pathway and a parallel PLX-2-independent pathway. The PLX-2-independent pathway might be active in the wild type or might be activated only in the absence of PLX-2. In the latter case, elimination of the parallel pathway alone would confer subtle phenotypes that are synthetic with *plx-2* mutations. EFN-4 might act in the PLX-2-independent pathway, or in both pathways, as its loss of function causes phenotypes almost as strong as those of *mab-20* null mutants.

The nature of the hypothesized MAB-20 receptor in the PLX-2-independent pathway remains unknown. It is unlikely that the only other *C. elegans* plexin, PLX-1, functions in MAB-20 signaling, as PLX-1 does not interact with MAB-20 physically or genetically (Fujii *et al.* 2002), and *plx-1 plx-2* double mutants do not exhibit ray fusion defects (S. Takagi, unpublished observations). We infer that MAB-20 must interact with a nonplexin receptor. Using mammalian cell culture, we have been unable to detect binding between MAB-20 and EFN-4; we also do not detect any effect of the coexpression of EFN-4 on the ability of PLX-2 to bind MAB-20 (S. Takagi, unpublished results). EFN-4 might act indirectly to stabilize or localize the hypothetical MAB-20 receptor, or it could perform a similar function for MAB-20 itself. However, our use of heterologous mammalian cells may preclude detecting any direct interactions if they are dependent on a coreceptor.

MAB-20 is a member of the "invertebrate-specific" class 2 semaphorins, whose signaling mechanisms remain less well studied. Drosophila expresses two class 2 semaphorins, Sema-2a and Sema-2b; Sema 2a is expressed by muscles, where it acts as a repellent in motor axon targeting in the neuromuscular system (Winberg *et al.* 1998). The Drosophila plexin PlexB has recently been shown to act as a receptor for Sema-2a (Ayoob *et al.* 2006). In contrast to our findings in *C. elegans*, in Drosophila the plexB phenotype is much more severe than the Sema-2a phenotype, implying that PlexB interacts with additional ligands, possibly Sema-2b or itself. Within the sensory nervous system, *sema2a* and *plexB* mutants display similar phenotypes, yet *sema2a plexB* double mutants are enhanced relative to the single mutants, suggesting involvement of additional ligands or receptors (Bates and Whitington 2007). Thus, current analysis of class 2 semaphorins has suggested some complexity of ligand–receptor relationships but has not yet provided clear instances of plexin-independent signaling. However, several vertebrate semaphorins can signal independently of plexins. The transmembrane semaphorin Sema 4D interacts with two quite different receptors: in the nervous system, Sema 4D interacts with a complex of PlexB1 and Met, whereas in the immune system it interacts with a lectin, CD72 (Kumanogoh *et al.* 2000). The latter interaction appears to be independent of a plexin receptor. Likewise, Sema 4A functions in T-cell development independently of plexins, instead binding the mucin-like protein Tim-2 (Kumanogoh *et al.* 2002). The cell surface semaphorin Sema 7A binds Plexin C1, but Plex C1 is not required for Sema 7A's function in promoting axon outgrowth, which is mediated by integrins (Pasterkamp *et al.* 2003). Unlike Sema 7A, MAB-20 lacks the Arg–Gly–Asp (RGD) motif and so is unlikely to interact with integrins.

Roles of plexin extracellular domains in semaphorin binding: Plexin extracellular domains contain an N-terminal sema domain and membrane-proximal MRS and GP domains. On the basis of structure–function analyses of plexin A1, plexins are thought to exist in an autoinhibited state in the absence of ligand due to an intramolecular interaction of the sema domain with the MRS and GP domains (Takahashi and Strittmatter 2001). Binding of semaphorin ligand to the plexin sema domain by sema–sema heterodimerization releases this autoinhibition, leading to a change in the conformation of the plexin intracellular domain and activation of intracellular pathways. It is not yet known to what extent this model for Plexin A applies to other plexins.

Our analysis of PLX-2/MAB-20 binding shows that, as expected, the PLX-2 sema domain is essential for interaction with semaphorin ligand, whereas the MRS and GP domains are essential for PLX-2 function, but not for MAB-20 binding. The *plx-2(nc7)* in-frame deletion of the MRS and GP domains enhances the phenotype of weak *mab-20* mutants to a degree comparable to that of a *plx-2* null mutation. Although the autoinhibition model suggests that deletion of MRS and GP domains should increase plexin activity, *plx-2(nc7)* behaves like a null mutation in this assay. This might be explained if the MRS and GP domains also played a role in plexin stability. In cell culture experiments, both PLX-2ΔMRS-GP and PLX-1ΔMRS-GP proteins are expressed, albeit at

lower levels than the full-length proteins. The loss of function in *plx-2(nc7)* mutants therefore suggests additional roles beyond stabilization for the MRS and GP domains. However, in our analysis of VNB migrations, *nc7* behaved differently from *tm729*. Whereas *tm729* results in a delay in VNB migrations relative to the wild type, *nc7* causes the VNBs to begin migration earlier than the wild type, suggesting that *nc7* may indeed result in a gain of function in this context. In contrast to PLX-2, we find that PLX-1ΔMRS-GP did not bind its semaphorin ligand, suggesting that the roles of the MRS and GP repeats may depend on the class of plexin. We do not know of other direct tests of the roles of the MRS and GP domains in plexin–semaphorin binding. The MRS domain of Plexin B1 is not required for it to associate with the Met receptor (Giordano *et al.* 2002); in the case of Met itself, internal deletion of the MRS domain was found to interfere with protein processing (Kong-Beltran *et al.* 2004), and thus the exact role of these domains remains uncertain.

MAB-20 signaling in ray development: Eph family receptor-type tyrosine kinases and their ligands, ephrins, mediate both adhesive and repulsive cell–cell interactions (Poliakov *et al.* 2004). *C. elegans* encodes a single Eph receptor, VAB-1 (George *et al.* 1998), and four ephrins, EFN-1–4. Previous analysis showed that EFN-4 is unlikely to act as a ligand for VAB-1, leaving open the question of how EFN-4 signals (Chin-Sang *et al.* 2002). The similarity of *mab-20* and *efn-4* phenotypes in VNB migration and male tail development and the lack of enhancement in double mutants suggested that they could affect a common process. Our analysis of the genetic interactions among *efn-4*, *mab-20*, and *plx-2* in embryogenesis provides additional evidence that EFN-4 acts in a MAB-20 pathway. Some phenotypes observed in *mab-20* mutants and not in *efn-4* mutants, such as the defects in late embryonic epidermal development, can now be ascribed to PLX-2 acting in parallel to EFN-4. As *efn-4* mutants display some additional phenotypes not observed in *mab-20* mutants, EFN-4 may act independently of MAB-20 in some situations.

The interactions between MAB-20 and EFN-4 in male tail-ray development have been examined in two other studies. Hahn and Emmons (2003) found that some ray fusions (rays 2 and 6) occurred more frequently in *mab-20; efn-4* double mutants than in the single mutants and concluded that EFN-4 and MAB-20 had independent roles in ray development. In contrast, Ikegami *et al.* (2004) concluded that EFN-4 accounted for "the bulk" of MAB-20 signaling in ray sorting. Our observations are more consistent with those of Ikegami *et al.* (2004), as we find that *mab-20 efn-4* double mutants display levels of ray fusion that are not significantly different from those of *mab-20* single mutants. A caveat to this interpretation is that *mab-20* single mutants display very highly penetrant ray fusions, so further enhancement in double mutants may be hard to detect or only significant with a larger sample size. Our analysis of Rn.p cell morphology, for which *mab-20* and *efn-4* single mutants have less penetrant defects and for which the double mutant is, overall, not enhanced relative to the strongest single mutant, supports the model that MAB-20 and EFN-4 have largely overlapping functions.

MAB-20-signaling pathways in VNB migration and epidermal morphogenesis may be different: In embryonic morphogenesis, *efn-4* and *mab-20* mutants display defects in ventral neuroblast migration that are not further enhanced in the double mutant. This is striking in light of the strong synergism of *efn-4* with other pathways involved in VNB movements, such as *vab-1* (Eph RTK), *ptp-3* (LAR RPTP), or *kal-1* (Kallmann syndrome protein/Anosmin-1) (Chin-Sang *et al.* 2002; Hudson *et al.* 2006). The specific lack of synergism between *mab-20* and *efn-4* in VNB migrations is consistent with their acting in a common pathway to promote VNB movement. In contrast, PLX-2 appears to play a relatively minor role in VNB migration. Although *plx-2* mutants display weak VNB migration defects, *plx-2* did not significantly enhance VNB migration defects of *efn-4*, *mab-20*, or *kal-1* null mutants. We conclude that the role of MAB-20 in VNB migration is more dependent on the putative PLX-2-independent pathway that involves EFN-4, consistent with the widespread expression of EFN-4 in ventral neuroblasts compared to PLX-2.

Our analysis of embryonic morphogenesis suggests that PLX-2 may have a specific, albeit redundant, function in mediating the epidermal cell-sorting functions of MAB-20. MAB-20 signaling prevents ectopic contacts between ventral epidermal cells (Roy *et al.* 2000). Such ectopic contacts presumably lead to a weakening of the epidermal layer and the late embryonic epidermal ruptures characteristic of *mab-20* mutants. In contrast, *efn-4* mutants do not display ectopic P-cell contacts nor do they rupture in elongation (Chin-Sang *et al.* 2002). This difference can now be accounted for if PLX-2 acts redundantly with EFN-4 in mediating the cell-sorting functions of MAB-20 within the epidermis.

Whereas in ventral neuroblast migration MAB-20 and EFN-4 appear to have similar roles, in later epidermal development they appear to partly antagonize, as *mab-20* epidermal rupture phenotypes are partly suppressed by *efn-4*. Finally, in male tail development, MAB-20 and EFN-4 again appear to play similar roles in promoting ray sorting. In interpreting these interactions, a central caveat is that in no case has it been demonstrated that the developmental defect results from a lack of adhesion or a lack of repulsion. However, defects in VNB migration are most simply explained as due to a lack of adhesion among VNB cells, whereas ectopic epidermal cell contacts and ray fusion defects are most simply explained as due to lack of repulsive interactions (Figure 8). We speculate that both MAB-20 and EFN-4, like other semaphorins and ephrins, can promote adhesion or repulsion, depending on the cellular context and the level

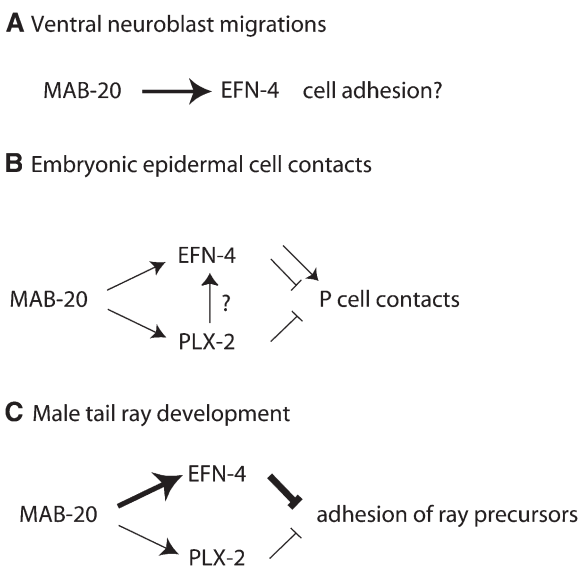

FIGURE 8.—Model for function of PLX-2 and EFN-4 in MAB-20 signaling. (A) In early embryonic movements of ventral neuroblasts, MAB-20 and EFN-4 may act in a common pathway that could promote adhesion between neighboring neuroblasts or between neuroblasts and unknown substrate cells. (B) In later embryonic development, MAB-20 prevents ectopic cell contacts between epidermal cells; EFN-4 and PLX-2 have redundant functions in this process. EFN-4 may also play an antagonistic role as the frequency of late embryonic arrest is reduced in *mab-20 efn-4* double mutants relative to *mab-20* single mutants. (C) In postembryonic development of male tail rays, MAB-20 and EFN-4 play nonredundant roles in preventing inappropriate adhesion of ray cells; PLX-2 plays a cryptic role that is revealed only in *mab-20* hypomorphic backgrounds.

of signaling. As EFN-4 appears to promote adhesion in ventral neuroblast migration in the absence of PLX-2, PLX-2 might modulate or upregulate EFN-4 signaling such that it promotes repulsion and not adhesion.

An important question is whether the apparent redundancy of PLX-2 in MAB-20 signaling reflects redundancy of PLX-2 with other pathways in the same cells or redundant roles of PLX-2 expressing and nonexpressing cells. Assuming that EFN-4 is a component of the redundant pathway, this may be addressed by comparing expression patterns of EFN-4 and PLX-2. EFN-4 and PLX-2 appear to be coexpressed in posterior epidermal cells in the late embryo, a context in which they have redundant roles in cell sorting, suggesting that EFN-4 and PLX-2 may act in the same cells to transduce a MAB-20 repellent or sorting signal. In other situations, such as ventral neuroblast migration, EFN-4 appears to act largely independently of PLX-2 and is not coexpressed with PLX-2. In ray development, EFN-4 and PLX-2 are coexpressed in some ray cell groups but not coexpressed in others. In conclusion, we suggest that MAB-20 interacts with distinct receptor complexes in different processes and that the composition of the receptor complex determines the effect of MAB-20 signaling on cell behavior. The complexity of the MAB-20 pathway and the involvement of ephrin signaling may have implications for other class 2 semaphorin pathways, and possibly for other vertebrate semaphorins for which the receptors have not been fully elucidated.

We thank Joe Culotti for communicating unpublished observations, Yuji Kohara for cDNA clones, Andrew Fire for GFP expression vectors, Ian Chin-Sang for the EFN-4 expression construct, Mizuno (Tohoku University) for pCEP-SYFcAP, Yoichi Oda for encouragement, and past and present members of our laboratories for discussion and advice throughout this work. We thank Y. Jin for use of her confocal microscope. Some strains were provided by the Caenorhabditis Genetic Center, which is funded by the U.S. National Institutes of Health (NIH) National Center for Research Resources. Work in A.D.C.'s laboratory was supported by the U.S. Public Health Service (NIH R01 GM54657). This work was supported by grants from the Ministry of Education, Science and Culture, Japan (H.F., S.T.); a grant from the National Bioresource Project of the Ministry of Education, Science and Culture, Japan (S.M.); and a grant from the Core Research for Evolutional Science and Technology of the Japan Science and Technology Corporation (H.F.).

LITERATURE CITED

AYOOB, J. C., J. R. TERMAN and A. L. KOLODKIN, 2006 Drosophila Plexin B is a Sema-2a receptor required for axon guidance. Development **133:** 2125–2135.

BAIRD, S. E., D. H. FITCH, I. A. KASSEM and S. W. EMMONS, 1991 Pattern formation in the nematode epidermis: determination of the arrangement of peripheral sense organs in the *C. elegans* male tail. Development **113:** 515–526.

BATES, K. E., and P. M. WHITINGTON, 2007 Semaphorin 2a secreted by oenocytes signals through plexin B and plexin A to guide sensory axons in the Drosophila embryo. Dev. Biol. **302:** 522–535.

BRENNER, S., 1974 The genetics of *Caenorhabditis elegans*. Genetics **77:** 71–94.

CHIN-SANG, I. D., S. E. GEORGE, M. DING, S. L. MOSELEY, A. S. LYNCH *et al.*, 1999 The ephrin VAB-2/EFN-1 functions in neuronal signaling to regulate epidermal morphogenesis in *C. elegans*. Cell **99:** 781–790.

CHIN-SANG, I. D., S. L. MOSELEY, M. DING, R. J. HARRINGTON, S. E. GEORGE *et al.*, 2002 The divergent C. elegans ephrin EFN-4 functions inembryonic morphogenesis in a pathway independent of the VAB-1 Eph receptor. Development **129:** 5499–5510.

CHISHOLM, A. D., and J. HARDIN, 2005 Epidermal morphogenesis, in *Wormbook*, edited by The *Caenorhabditis elegans* Research Community. http://www.wormbook.org.

DALPE, G., L. W. ZHANG, H. ZHENG and J. G. CULOTTI, 2004 Conversion of cell movement responses to Semaphorin-1 and Plexin-1 from attraction to repulsion by lowered levels of specific RAC GTPases in C. elegans. Development **131:** 2073–2088.

DALPE, G., L. BROWN and J. G. CULOTTI, 2005 Vulva morphogenesis involves attraction of plexin 1-expressing primordial vulva cells to semaphorin 1a sequentially expressed at the vulva midline. Development **132:** 1387–1400.

EVAN, G. I., G. K. LEWIS, G. RAMSAY and J. M. BISHOP, 1985 Isolation of monoclonal antibodies specific for human c-myc proto-oncogene product. Mol. Cell. Biol. **5:** 3610–3616.

FAN, J., S. G. MANSFIELD, T. REDMOND, P. R. GORDON-WEEKS and J. A. RAPER, 1993 The organization of F-actin and microtubules in growth cones exposed to a brain-derived collapsing factor. J. Cell Biol. **121:** 867–878.

FUJII, T., F. NAKAO, Y. SHIBATA, G. SHIOI, E. KODAMA *et al.*, 2002 Caenorhabditis elegans PlexinA, PLX-1, interacts with transmembrane semaphorins and regulates epidermal morphogenesis. Development **129:** 2053–2063.

FUJISAWA, H., K. OHTA, T. KAMEYAMA and Y. MURAKAMI, 1997 Function of a cell adhesion molecule, plexin, in neuron network formation. Dev. Neurosci. **19:** 101–105.

GENGYO-ANDO, K., and S. MITANI, 2000 Characterization of mutations induced by ethyl methanesulfonate, UV, and trimethylpsoralen

in the nematode Caenorhabditis elegans. Biochem. Biophys. Res. Commun. **269:** 64–69.

George, S. E., K. Simokat, J. Hardin and A. D. Chisholm, 1998 The VAB-1 Eph receptor tyrosine kinase functions in neural and epithelial morphogenesis in *C. elegans*. Cell **92:** 633–643.

Gherardi, E., C. A. Love, R. M. Esnouf and E. Y. Jones, 2004 The sema domain. Curr. Opin. Struct. Biol. **14:** 669–678.

Ginzburg, V. E., P. J. Roy and J. G. Culotti, 2002 Semaphorin 1a and semaphorin 1b are required for correct epidermal cell positioning and adhesion during morphogenesis in C. elegans. Development **129:** 2065–2078.

Giordano, S., S. Corso, P. Conrotto, S. Artigiani, G. Gilestro *et al.*, 2002 The semaphorin 4D receptor controls invasive growth by coupling with Met. Nat. Cell Biol. **4:** 720–724.

Hahn, A. C., and S. W. Emmons, 2003 The roles of an ephrin and a semaphorin in patterning cell-cell contacts in C. elegans sensory organ development. Dev. Biol. **256:** 379–388.

Hinck, L., 2004 The versatile roles of "axon guidance" cues in tissue morphogenesis. Dev. Cell **7:** 783–793.

Hu, H., T. F. Marton and C. S. Goodman, 2001 Plexin B mediates axon guidance in Drosophila by simultaneously inhibiting active Rac and enhancing RhoA signaling. Neuron **32:** 39–51.

Hudson, M. L., T. Kinnunen, H. N. Cinar and A. D. Chisholm, 2006 *C. elegans* Kallmann syndrome protein KAL-1 interacts with syndecan and glypican to regulate neuronal cell migrations. Dev. Biol. **204:** 352–365.

Ikegami, R., H. Zheng, S. H. Ong and J. Culotti, 2004 Integration of semaphorin-2A/MAB-20, ephrin-4, and UNC-129 TGF-beta signaling pathways regulates sorting of distinct sensory rays in C. elegans. Dev. Cell **6:** 383–395.

Isbister, C. M., A. Tsai, S. T. Wong, A. L. Kolodkin and T. P. O'Connor, 1999 Discrete roles for secreted and transmembrane semaphorins in neuronal growth cone guidance in vivo. Development **126:** 2007–2019.

Isbister, C. M., P. J. Mackenzie, K. C. To and T. P. O'Connor, 2003 Gradient steepness influences the pathfinding decisions of neuronal growth cones in vivo. J. Neurosci. **23:** 193–202.

Kameyama, T., Y. Murakami, F. Suto, A. Kawakami, S. Takagi *et al.*, 1996a Identification of a neuronal cell surface molecule, plexin, in mice. Biochem. Biophys. Res. Commun. **226:** 524–529.

Kameyama, T., Y. Murakami, F. Suto, A. Kawakami, S. Takagi *et al.*, 1996b Identification of plexin family molecules in mice. Biochem. Biophys. Res. Commun. **226:** 396–402.

Kolodkin, A. L., D. J. Matthes and C. S. Goodman, 1993 The semaphorin genes encode a family of transmembrane and secreted growth cone guidance molecules. Cell **75:** 1389–1399.

Kong-Beltran, M., J. Stamos and D. Wickramasinghe, 2004 The Sema domain of Met is necessary for receptor dimerization and activation. Cancer Cell **6:** 75–84.

Kozak, M., 1992 Regulation of translation in eukaryotic systems. Annu. Rev. Cell Biol. **8:** 197–225.

Kruger, R. P., J. Aurandt and K. L. Guan, 2005 Semaphorins command cells to move. Nat. Rev. Mol. Cell Biol. **6:** 789–800.

Kumanogoh, A., C. Watanabe, I. Lee, X. Wang, W. Shi *et al.*, 2000 Identification of CD72 as a lymphocyte receptor for the class IV semaphorin CD100: a novel mechanism for regulating B cell signaling. Immunity **13:** 621–631.

Kumanogoh, A., S. Marukawa, K. Suzuki, N. Takegahara, C. Watanabe *et al.*, 2002 Class IV semaphorin Sema4A enhances T-cell activation and interacts with Tim-2. Nature **419:** 629–633.

Liu, Z., T. Fujii, A. Nukazuka, R. Kurokawa, M. Suzuki *et al.*, 2005 C. elegans PlexinA PLX-1 mediates a cell contact-dependent stop signal in vulval precursor cells. Dev. Biol. **282:** 138–151.

Maeda, I., Y. Kohara, M. Yamamoto and A. Sugimoto, 2001 Large-scale analysis of gene function in Caenorhabditis elegans by high-throughput RNAi. Curr. Biol. **11:** 171–176.

Maestrini, E., L. Tamagnone, P. Longati, O. Cremona, M. Gulisano *et al.*, 1996 A family of transmembrane proteins with homology to the MET-hepatocyte growth factor receptor. Proc. Natl. Acad. Sci. USA **93:** 674–678.

Matthes, D. J., H. Sink, A. L. Kolodkin and C. S. Goodman, 1995 Semaphorin II can function as a selective inhibitor of specific synaptic arborizations. Cell **81:** 631–639.

Niwa, H., K. Yamamura and J. Miyazaki, 1991 Efficient selection for high-expression transfectants with a novel eukaryotic vector. Gene **108:** 193–199.

Ohta, K., S. Takagi, H. Asou and H. Fujisawa, 1992 Involvement of neuronal cell surface molecule B2 in the formation of retinal plexiform layers. Neuron **9:** 151–161.

Ohta, K., A. Mizutani, A. Kawakami, Y. Murakami, Y. Kasuya *et al.*, 1995 Plexin: a novel neuronal cell surface molecule that mediates cell adhesion via a homophilic binding mechanism in the presence of calcium ions. Neuron **14:** 1189–1199.

Pasterkamp, R. J., and A. L. Kolodkin, 2003 Semaphorin junction: making tracks toward neural connectivity. Curr. Opin. Neurobiol. **13:** 79–89.

Pasterkamp, R. J., J. J. Peschon, M. K. Spriggs and A. L. Kolodkin, 2003 Semaphorin 7A promotes axon outgrowth through integrins and MAPKs. Nature **424:** 398–405.

Poliakov, A., M. Cotrina and D. G. Wilkinson, 2004 Diverse roles of eph receptors and ephrins in the regulation of cell migration and tissue assembly. Dev. Cell **7:** 465–480.

Portman, D. S., and S. W. Emmons, 2000 The basic helix-loop-helix transcription factors LIN-32 and HLH-2 function together in multiple steps of a C. elegans neuronal sublineage. Development **127:** 5415–5426.

Puschel, A. W., R. H. Adams and H. Betz, 1995 Murine semaphorin D/collapsin is a member of a diverse gene family and creates domains inhibitory for axonal extension. Neuron **14:** 941–948.

Rohm, B., B. Rahim, B. Kleiber, I. Hovatta and A. W. Puschel, 2000 The semaphorin 3A receptor may directly regulate the activity of small GTPases. FEBS Lett. **486:** 68–72.

Roy, P. J., H. Zheng, C. E. Warren and J. G. Culotti, 2000 *mab-20* encodes Semaphorin-2a and is required to prevent ectopic cell contacts during epidermal morphogenesis in *Caenorhabditis elegans*. Development **127:** 755–767.

Semaphorin Nomenclature Committee, 1999 Unified nomenclature for the semaphorins/collapsins. Cell **97:** 551–552.

Shibata, Y., T. Fujii, J. A. Dent, H. Fujisawa and S. Takagi, 2000 EAT-20, a novel transmembrane protein with EGF motifs, is required for efficient feeding in *Caenorhabditis elegans*. Genetics **154:** 635–646.

Simmer, F., M. Tijsterman, S. Parrish, S. P. Koushika, M. L. Nonet *et al.*, 2002 Loss of the putative RNA-directed RNA polymerase RRF-3 makes C. elegans hypersensitive to RNAi. Curr. Biol. **12:** 1317–1319.

Suchting, S., R. Bicknell and A. Eichmann, 2006 Neuronal clues to vascular guidance. Exp. Cell Res. **312:** 668–675.

Swiercz, J. M., R. Kuner, J. Behrens and S. Offermanns, 2002 Plexin-B1 directly interacts with PDZ-RhoGEF/LARG to regulate RhoA and growth cone morphology. Neuron **35:** 51–63.

Takahashi, T., and S. M. Strittmatter, 2001 Plexina1 autoinhibition by the plexin sema domain. Neuron **29:** 429–439.

Takegahara, N., A. Kumanogoh and H. Kikutani, 2005 Semaphorins: a new class of immunoregulatory molecules. Philos. Trans. R. Soc. Lond. B Biol. Sci. **360:** 1673–1680.

Tamagnone, L., S. Artigiani, H. Chen, Z. He, G. I. Ming *et al.*, 1999 Plexins are a large family of receptors for transmembrane, secreted, and GPI-anchored semaphorins in vertebrates. Cell **99:** 71–80.

Vikis, H. G., W. Li, Z. He and K. L. Guan, 2000 The semaphorin receptor plexin-B1 specifically interacts with active Rac in a ligand-dependent manner. Proc. Natl. Acad. Sci. USA **97:** 12457–12462.

Winberg, M. L., J. N. Noordermeer, L. Tamagnone, P. M. Comoglio, M. K. Spriggs *et al.*, 1998 Plexin A is a neuronal semaphorin receptor that controls axon guidance. Cell **95:** 903–916.

Communicating editor: K. Kemphues